Chinese Chemical Letters 35 (2024) 109381

Contents lists available at ScienceDirect

Chinese Chemical Letters

journal homepage: www.elsevier.com/locate/cclet

Metal organic framework modulated nanozymes tailored with their biomedical approaches

Manoj Kumar Sarangi[a,*], L.D Patel[b], Goutam Rath[c], Sitansu Sekhar Nanda[d], Dong Kee Yi[d]

[a] Department of Pharmaceutics, Amity Institute of Pharmacy, Amity University, Lucknow 201313, India
[b] Department of Pharmaceutics, Parul Institute of Pharmacy, Parul University, Vadodara 391760, India
[c] Department of Pharmaceutics, School of Pharmaceutical Sciences, Siksha 'O' Anusandhan University, Bhubaneswar 751030, India
[d] Department of Chemistry, Myongji University, Yongin 03674, Republic of Korea

ARTICLE INFO

Article history:
Received 28 August 2023
Revised 29 November 2023
Accepted 4 December 2023
Available online 12 December 2023

Keywords:
MOF
Nanozyme
Catalysis
Biomedicine
Theranostics

ABSTRACT

Nanozymes are the paradigm for bridging inorganic nanomaterials with biology and environment for taking the spontaneous responsibilities to outplay natural enzymes. Metal-organic frameworks (MOFs) are mesoporous materials of inorganic-organic coordination, bearing ampoules of active/target sites and having the tendency to mimic natural enzymes. Thus MOF-based nanozymes (NZs) could be recognized for their tremendous potential for bio-catalysis. However, MOFs are of four types namely: modified MOFs, pristine MOFs, MOF-derived materials and MOFs comprised of natural enzymes. The MOFs-based NZ modulated *via* ultrasound, light, and heat revealed diversified applications. This article is concentrated on different methods for the preparation of MOF-based NZ for mimicking the responses of catalases, multifunctional enzymes, oxidases, superoxide dismutase, hydrolases, and peroxidases, progress and challenges of MOFs/MOF-based materials for exploiting their recent and futuristic approaches in biomedical sector.

1. Introduction

Despite of the potential impacts (brilliant biocatalysts), natural enzymes (NEs) are facing difficulty with their production and scale-up (because of poor stability, expensiveness and complex synthetic procedures) resulting in the search for substitutions [1]. The stability and the catalytic responsiveness of NEs considerably declined at the extreme temperature and pH conditions [2]. Due to stringency in purification and preparation of NEs, they seem to be very much costly. Conversely, nanozymes (NZs) are found to be the specific alternatives with tremendous intrinsic catalytic responses revealing with a considerable prolonged stability, and composition/size dependent affinity [2]. The larger surface areas provided with NZs further facilitates some essential modifications followed by bio conjugation and nano incorporation [3]. The concept of NZ got popularized in 2007 with the advent of Fe_2O_3 nanoparticles (NPs) resembling peroxidase-like activity [4,5] and further explored with nanomaterials as potential enzymes in different research outcomes [6]. NZ are defined as metal oxides [7–10], carbon-metal nanomaterials [11,12], NPs [7], along with their composites revealing enzyme-like responses [13]. Within a span of 16 years, over 320 types of NZ have been reported by 300 laboratories globally, which seems to be a paramount achievement in the segment of bio-catalysis and turned out to be a crucial alternative to the natural ancestors with eco-friendly, and diversified applications [14–25]. The approach of nanozyme leads to the development of more stable and recyclable biocatalysts in accelerated pressure and temperature condition [26–30]. With some crucial surface modifications, such elements are actively imparting antibacterial activity, potentially explored as biosensors and useful in cancer theranostics [31,32]. Regardless of the superiority of NZ over natural ones, the NZ are greatly constrained with their intrinsic catalytic activities because of the reduced number of active sites, aggregation tendency and lack of multilevel structure. In order to overcome such discrepancies, metal-organic frameworks (MOFs) as well as their respective derivatives were envisioned for exploring the research arena [32].

MOFs are the class of mesoporous crystalline materials, structurally oriented *via* self-assembled organic ligands and ions of transitional metal. The MOFs are usually enabled by biocatalysis of drugs and their release. However, the physiological degradation of MOF as well as MOF-mediated composites (like MOF/enzyme, MOF/SiO_2, and MOF/Ag composites) may lead to inhibiting the dissolution rate of some drugs/elements. Therefore, MOF-based derivatives (like metal oxides/carbon NPs, oxides/carbon NPs, nano-

* Corresponding author.
E-mail address: manojsarangi2007@rediffmail.com (M.K. Sarangi).

https://doi.org/10.1016/j.cclet.2023.109381
1001-8417/

materials from metal/carbon and carbon-based nanomaterials) could be developed to overcome such issues [33–40]. The MOFs could be further of several types such as: (1) Isoreticular MOFs: These are microporous octahedral crystalline materials usually synthesized by a series of aromatic carboxylates as well as $[Zn_4O]^{6+}$ SBU. It was reported that, the synthetic nanosheets of IRMOF-3 is highly efficient with utmost selectivity/sensitivity for recognizing 2,4,6-trinitrophenol for wastewater management [41,42]. (2) Zeolitic imidazolate frameworks (ZIFs): Zeolitic imidazolate frameworks comprised of ZIF-90, ZIF-8, ZIF-71, ZIF-L, ZIF-7, and ZIF-67 [43]. They contains imidazole derivatives showing valence electrons. They revealed maximum acid sensitivity, lower cytotoxicity, showing greater surface area, and massive pore size [44]. The MOF- ZIF-8 designed by Pan and co-workers are highly involved in detection of the DNA of HIV-1 [45]. A substantial pore size along with the marvellous chemo-thermal stability of ZIFs are reflecting a benchmark for development of networks for generating novel MOF composites [46,47]. (3) Porous coordination networks (PCNs): PCNs like PCN-224, PCN-222, PCN-333, and PCN-57 are the 3D stereo-octahedron materials, with a surface topology of hole−cage−hole pattern [43]. Among the above types, PCN-222 MOF has been extensively exploited in designing of electrochemical sensor for DNA detection [48]. (4) Materials institute lavoisier (MIL) MOFs: MIL-MOFs comprised of MIL-100, MIL-101, MIL-88, MIL-53, and MIL-125 under elemental synthesis revealed valence electrons along with two carboxylic functional groups [43,49]. (5) Porous coordination polymers (PCPs): They are the synthesized either by pyridine or by carboxylic acid [43]. The first 3D network assembly of Prussian blue was synthesized by Ludi *et al*. [50]. Similarly, PCP Zn(NO2-ip)(bpy) was immobilized on QCM surface for sensing the organic vapours [51] and bio-macromolecular separation [52,53]. (6) University of Oslo (UiO) MOFs: The dicarboxylic acid based UiO-MOF such as Zr6 (μ^3-O)4(μ^3-OH) as SBU and PBU was synthesized for the first time by Lillerud *et al*. [54]. UiO-66(Zr) was developed from BDC and $ZrCl_4$ *via* solvothermal technique through tetrahedral and octahedral pore cages [54]. UiO-66 revealed a superb thermodynamic stability at an extreme pH condition (at pH 14) and can successfully be implemented as a super capacitor electrode material [44]. Meanwhile, numerous MOFs, such as, Pohang University of Science and Technology (POST-n) [55], Northwestern University (NU) [56], University of Nottingham (NOTT-n) [57], Dresden University of Technology (DUT-n family) [58], Christian-Albrechts-University (CAU-n family) [59], and Hong Kong University of Science and Technology (HKUST-n) [60], have recently emerged [61] with specifically deployed in several bio assisted approaches [62]. It has been reported that MOFs like MIL-88, MIL-53, MIL-101 and MIL-100 have revealed superior catalytic efficacy [40,63]. MOFs are further modified with metal NPs for exploiting their distinct structure [22,64] and metal oxide [65] leads to an enhanced catalytic response. Natural enzymes entrapped into the networking of MOF-based materials play a pivotal catalytic response at diverse microenvironments with utmost stability [66,67] compared to their pristine MOFs. The derivatives of MOF (based on metal oxides and porous carbon materials) can also be developed/synthesized *via* etching [40] and pyrolysis [68–74] for mimicking miscellaneous responses [75–77]. Despite the synthetic inorganic versions, MOFs could also be existing as MOF nanosheets and polyhedral MOFs with altered shapes and sizes [78]. The MOFs are also explored for the detection of several bio elements such as glutathione (GSH) [79] and glucose [80]. However, microenvironments such as temperature, pH and the concentration of H_2O_2 along with several stimuli for example ultrasound, magnetic fields, light and, heat leads to impact the catalytic efficacy of MOF-modulated NZ [81–89].

The current review is summarized with the development of numerous MOF-modulated NZ and their resemblance towards the responses of superoxide dismutases (SODs), peroxidases, catalases, oxidases, and multi-functional enzymes. We also have discussed various biomedical approaches of MOF-based nanomaterials such as anti-bacterial, sensing, anti-inflammatory and wound healing responses, Imaging, gene therapy, diabetes and chemotherapy.

2. Preparation of MOF-modulated nanozymes

The MOFs repeatedly endowed with metal nodes and/or organic ligands turns their catalytic response abundantly towards manageable enzymatic activities. The multilevel porosity enables tremendous connection within the substrates *vs.* active sites, revealing an unstoppable diffusion as well as the product transmission [90]. Moreover, the uniformity in size followed by the channel shaping of MOFs make them specific to be involved for size-oriented catalytic responses. Hence, MOFs and MOF derived enzyme responses make a unique portfolio with respect to their approaches [90]. Numerous methodologies were being reported earlier for development of MOF-modulated NZ. The unmodified pristine MOFs denoted limited catalytic activity up to a certain extent with a single application and followed a simplified synthetic procedure. For example, the solution of $FeCl_3{\cdot}6H_2O$ (in DMF) on addition with TA developed MIL-53 with continuous mixing for half an hour [91]. Similarly, the combination of HEPES buffer (at pH 8.0 and 10 mmol/L, in 700 mL), H3BTC (25 mmol/L, 200 mL), and $CuCl_2$ (50 mmol/L, 100 mL) at room temperature resulted in the development of Cu/H3BTC MOF [92]. Such limitations can be overcome by mounting NZ derived from MOFs, modified MOF materials, and MOF@natural enzymes.

2.1. Oxidases

Oxidase (OXD) a big bow in the enzyme category that used to catalyse a redox reaction where molecular O_2 is acting as electron acceptor towards substrates oxidation. Among various OXD, cytochrome c OXD, nicotinamide adenine dinucleotide phosphate OXD, glucose OXD, cytochrome P450, monoamine OXD, and sulfhydryl OXD are name a few those leads to oxidation of thiol groups. Rossi *et al*. revealed that AuNPs showed the property of glucose OXD in presence of O_2 [93] Similarly, Chen *et al*. reported the development of UMOF@Au through the integration of ultrasmall Au NZs + NPs coated with Zr/Fe-MOF [94]. Further it was denoted that, the developed UMOF@Au NZ has potentiated the impact of nanoreactor towards an effective cascade of biocatalysis for the generation of singlet oxygen ($^1O_2$) under the near infrared (NIR) irradiation. Wu *et al*. has fabricated MIL53(Fe)-X series (X = CH_3, NH_2, H, F, OH, Br, NO_2 and Cl) MOF-based NZs *via* the substitution of H atom in 1,4-benzenedicarboxylic acid ligand [95]. Among the developed NZs, MIL-53(Fe)-NO_2 was found to be exhibited with a 10-fold better OXD-mimicking response than those of the unsubstituted MIL-53(Fe) because of a strong electronegative impact of –NO_2 [90]. The materials growth (*in-situ*) on MOFs is considered to be one of the interesting preparation methods for modified MOF, where the MOF structural framework affects the propagation of stable NPs by reducing their aggregation rate [96]. The camptothecin-loaded Au nanocomposites were developed by exploring Fe-modulated MOF (*in-situ*) surface towards chemotherapy [96]. MOF modified with PEG-SH (methoxy–polyethene glycol thiol) and 1-dodecanethiol (C12SH) signified better stability [97]. Au NPs deposited over Cu-MOF-modulated electrode of glassy carbon *via* potentiostatic method dignified its miraculous catalytic activity towards nitrite along with potential electrical conductivity [98]. The development of polyoxometalate NPs and zeolitic imidazolate frameworks (ZIF) *via* the co-precipitation method showed a brilliant electrocatalytic ability along with marvellous oxygen evolution reaction accorded with long-term stability [99]. Pyrolysis is

also considered one of the popular techniques for developing MOF-based NZ to impart better catalytic response. Ce-MOFs under pyrolysis generated CeO_2 NPs, which leads to developing oxidase-like activity [85]. In another study, one-pot pyrolysis has opted to design Co and N-doped NZ by using ZIF-67 (precursor) [100–102]. Enzyme immobilization in MOFs (MOF-based encapsulation) denoted induced reactivity compared with the free enzymes, thus gaining greater popularity [103]. Zhao *et al*. suggested boric-acid-functionalized MOFs (hierarchical porous MOF (MIL-88B) as a carrier towards glucose oxidase [104]. Similarly, Fe-MIL-88B-NH_2 encapsulate glucose oxidase to reveal peroxidase-like activity, by offering better stability compared to the free enzyme [105,106].

2.2. Peroxidases

Peroxidase (POD) are the group of enzymes leads to catalyze substrates oxidation in presence of organic peroxides (R–OOH) or H_2O_2. Yan *et al*. revealed the POD-mimicking activity of Fe_3O_4, where the natural POD sites are widely occupied by multivalent metal ions (Fe^{2+}/Fe^{3+}, Mn^{2+}/Mn^{3+}, or Cu^{+}/Cu^{2+}) to facilitate reaction [107,108]. Hence, MOF-based NZs are of a great choice for mimicing the POD (H_2O_2 on surface adsorption over MOFs leads to catalysis of peroxy bond for generating hydroxyl radicals (OH)). In another instance, Zhao *et al*. revealed the fluorescence detection of dopamine (*via* POD mimicking and catalysis of H_2O_2 modulated OH to accelerate Fenton reaction for a better fluorescence effect) by using Fe-MIL-88 as a novel sensor [109]. Ranji-Burachaloo *et al*. carried out a MIL-88B (Fe)–NH_2 mediated partial reduction of Fe^{3+} into Fe^{2+} *via* hydrothermal method and further catalyze the generation of OH *via* heterogeneous/homogeneous catalysis [110]. Further, Wei *et al*. reported a brilliant performance of ultrathin MOF nanosheets over a bulk MOF analog [111]. Lin *et al*. has proposed the formation of Fe–N–C SAEs through pyrolysis of Fe–Zn-MOF at a very high-temperature [112]. POD usually catalyses H_2O_2 reactions over varied substrates. Numerous MOF-based NZ (with suitable modifications) being developed for mimicking the peroxidase-like NZ. Fu *et al*. developed the nanocube (Zr-Mn MOF) *via* hydrothermal process (one-pot) revealing an excellent peroxidase activity thereby promoting the conversion of H_2O_2 to –OH [113]. Zhang *et al*. synthesized PtAu/ZIF-8-rGO (abridged graphene oxide) NZ, which was proven to be an excellent H_2O_2 detector in human serum [114]. Similarly, Fe3O4/MIL-101(Fe) and Fe-based MOF (NH_2-MIL-88B(Fe)) developed by Jiang *et al*. and He *et al*., *via* ultrasonic-assisted electrostatic self-assembly technology and microwave heating respectively, catalyses the dimerization of o-phenyl enediamine and H_2O_2; highly susceptible towards magnetic fields [115,116]. Fe-modulated MOFs derived from hydroxyapatite nanowires (ultra-long) were utilized for developing a nucleate MOF nanofibers-based hydroxy–phosphorous limestone [83,117]. Phenyl selenyl bromide grafted on UIO-66-NH_2 (a Zr-modulated MOF) was applicable as energy donors and showed better catalytic response [80]. MOF NZ based on particles of Prussian blue, imparted a catalytic response with a magnitude of four times higher than the natural peroxidase [118,119]. Different techniques for preparation for numerous MOF-modulated nanozymes were stated in Table 1 [4].

2.3. Catalases

Catalase (CAT) was responsible for the decomposition of H_2O_2 into H_2O and O_2 thus protecting the cells from oxidative damage. Tsung *et al*. revealed the synthesis of CAT@MOF *via* de novo approach [120] with the help of ZIF-90 ([Zn(ica)^2], ica = 2-imidazolecarboxaldehyde) MOF maintaining a smaller size than that of the enzymes [121]. The developed CAT@MOF denoted an elevated chemo-thermal stability along with protection against proteinase K. NZs with CAT-mimicking response gets encapsulated easily [122,123] Wang *et al*. reported a MOF-modulated NZs *via* pyrolysis of analog $Mn_3[Co(CN)_6]_2$ and Prussian blue under aerobic conditions [124]. The mesoporous NZs of CAT were predominantly associated with NIR irradiation, and enhanced PDT efficacy in both *in vivo* and *in vitro* conditions [90]. The decomposition of H_2O_2 *via* MOF-based materials simulates catalases, thereby resulting in the formation of O_2, which could be applicable for photodynamic therapy (PDT). Liu *et al*. developed a MOF encapsulated with black phosphorus quantum dots and catalase on both exterior as well as interior surfaces and was responsible for converting H_2O_2 to O_2 thereby accelerating the production of $^1O_2$ [125]. Similarly, Yang *et al*. developed the formation of Pt NPs of the reduced size range in MOF-derived carbon NZ, thereby modulating the endogenous catalysis of H_2O_2 for generating O_2 [126,127].

2.4. Superoxide dismutases

Superoxide dismutase (SOD) is a brilliant antioxidant usually found in several plants, animals, and microbiotas which protects the internal cells/tissues from the oxidative stress mediated damage. Usually multivalent metal ions such as Cu^{2+}, $Fe^{3+/2+}$, $Ni^{3+/2+}$ and $Mn^{3+/2+}$ are having the tendency to showcase SOD-mimicking activity. Qu *et al*. developed ultrasmall Cu-TCPP MOF-based nanodots (TCPP = tetrakis(4-carboxyphenyl) porphyrin) with SOD-mimicking activity [128,129]. The prepared nanodots exhibited equivalent size to that of the natural enzymes, along with revealing more accessible catalytic sites towards the substrates followed by a faster diffusion tendency with a smart renal clearance to manage toxicity. Thus, the outcome of the research was further denoting an admiring response (*in vitro*/*in vivo*) by the NZs that leads to alleviate an acute renal injury with a safe and efficient way [90]. Numerous inflammatory processes associated with the human body lead to the overproduction of superoxide dismutase, resulting in the instigation of several resident immune cells thereby perpetrating the damage of organ and secondary tissues. SOD is a particular enzyme system responsible for regulating the equilibrium condition by preventing the catalysis of free radicals of superoxide to form H_2O_2 and O_2 [130]. Zhang *et al*. developed MOF dots of Cu-5,10,15,20-tetrakis(4-carboxyphenyl)porphyrin (TCPP) *via* a liquid exfoliation approach that leads to mimics the effect of SOD for controlling reactive oxygen species (ROS) level and preventing inflammations [130]. NPs of Prussian blue (PBNPs) mimicking SOD activity slaked free radicals of superoxide (O_2^-) at a varied pH level [130].

2.5. Hydrolases

Hydrolases are the class of transferases enzymes used for catalysing hydrolysis. Soybean epoxy hydrolase (SEH) *via* cross-linking and precipitation was mounted over the surface of UIO-66-NH_2 MOF. The resulting nanozyme (SEH@UiO-66-NH_2) was configured with SEH loading of 87.3 mg/g and showed responsiveness of 88% higher than that of free SEH along with thermos-stability, stability in diversified pH, and a better chemical tolerance towards several organic solvents [131].

2.6. Glutathione peroxidase

Glutathione peroxidase (GPx) is considered as another versatile oxidation–reduction enzyme that usually protects the organism from oxidative stress/damage [132]. Despite of the tremendous prosperity of GPx towards the management of intracellular redox homeostatis, it usually faces some common issues like poor bioavailability and low stability. However, NZs offer extraordinary responses for boosting up the impact of GPx. The GPx-mimicking

Table 1
Preparation techniques for various MOF-based nanozymes.

Enzymes	Materials	Classifications	Preparations
Peroxidase	Mn–Zr MOF	Modified MOF	One-pot hydrothermal process
	AuPt/ZIF-8-rGO	Modified MOF	Simple wet chemical process and *in situ*-reduction
	Fe_3O_4/MIL-101(Fe)	Modified MOF	Ultrasonic-assisted electrostatic self-assembly technology
	NH_2-MIL-88B(Fe)	Modified MOF	Microwave heating
	HAP@MIL-100(Fe)	Modified MOF	Template method
	Prussian blue particles	Unmodified MOF	H_2O_2 catalytic activation
	PB/MIL-101(Fe)	Modified MOF	*In-situ* growth
	Co_3O_4@Co-Fe oxide DSNCs	MOF derivatives	*In-situ* growth
Oxidase	Au/FeMOF@CPT	Modified MOF	Simple wet method
	Au@Cu-MOF	Modified MOF	Co-precipitation
	ZIF-8@ZIF-67@POM	Modified MOF	One-pot pyrolysis
	CeO_2	MOF derivatives	One-pot pyrolysis
	Co,N-HPC	MOF derivatives	Simple pyrolysis
	Fe–N/C	MOF derivatives	Solvothermal method and pyrolysis
	C-CoM-HNC	MOF derivatives	–
	GOx@HP-MIL-88B-BA	MOF@natural enzymes	Amidation coupling reaction
	GOx@Fe-MOF	MOF@natural enzymes	–
	GOx@MOF-545(Fe)	MOF@natural enzymes	–
	LDH@NU-100x	MOF@natural enzymes	–
SOD	Cu-TCPP MOF dots	Modified MOF	Liquid exfoliation
Catalase	BQ-MIL@cat-MIL	Modified MOF	*In-situ* growth
	Pt-C	MOF derivatives	*In-situ* reduction
Oxidase and peroxidase	Au/Cu-TCPP(M)	Modified MOF	*In-situ* growth
	MOF(Co/2Fe)	Modified MOF	Hydrothermal method
	Ce-BPyDC	Modified MOF	Hydrothermal method
Soybean epoxy hydrolase	SEH@UiO-66-NH	Modified MOF	Precipitation and cross-linking
Reductase	Fe–N–C	MOF derivatives	Thermal conversion
	Co–Fe alloy@N-doped carbon hollow spheres	MOF derivatives	Pyrolysis
	Carbon nanotubes	MOF derivatives	Pyrolysis

Note: GOx: glucose oxidase; LDH: lactate dehydrogenase; HAP: hydroxyapatite.

NZs responses are governed *via* generation of MnO_2 nanoparticles, that leads to catalyses the oxidation of GSH to GSSG followed by conversion of Mn^{4+} into Mn^{2+} [133]. Numerous metal oxides those are associated with the mimicking responses for GPx include V_2O_5, Mn_3O_4, and CeO_2. Very recently, By applying the engineered ligand strategy Wei *et al*. revealed a tailored response towards GPx-mimicking over MIL-47(V)-X MOF-based NZs *via* substitution of H atom by Br, F, CH_3, OH, and NH_2 groups in 1,4-benzenedicarboxylicacid ligand [134] to develop MIL-47(V)-Br, MIL-47(V)-F, MIL-47(V)-CH_3 and MIL-47(V)-NH_2. Among the developed NZs, the isostructural MIL-47(V)-NH_2 and MIL-47(V)-X MOFs, exhibited optimum GPx-mimicking responses followed by excellent (*in vitro* and *in vivo*) anti-inflammatory responses [90].

2.7. Multi-modal enzymes

Such types of NZ is considered the hybrid enzyme system which is usually developed by combining multiple enzymes in lieu of their catalytic activity. The glucose oxidase enabled ZIF-8 MOF added to Fe-PDA (iron–polydopamine shell) resulted with an indulged impact of a dual enzyme system (glucose oxidase and peroxidase) for a better chemical stability [135]. Similarly, the development of a hybrid nanosheet (comprising of ultrafine-Au NPs frilled over a nanosheet of 2D metal-porphyrin MOF (*in situ*)), Ce-MOF, and a bimetallic (Fe and Co) doped MOFs revealed both oxidase and peroxidase-like activity [136–138].

3. Advances in different MOF-based nanozymes

3.1. MOF-derived M–N–C nanozymes

Numerous MOF-derived carbon nanostructures (mesoporous) were developed by using MOF derivatives as precursors [139]. Because of MOFs diversifications, carbonization was usually carried out in varied gaseous environments like argon, hydrogen, and nitrogen with specific control over temperature to obtain carbon-based formulations like pure carbon, alloy/carbon, and heterogeneous atoms doped with carbon (NZ like carbon dots, fullerene, graphene oxide, carbon nanotubes, and carbon nitride) to denote better catalytic response [140,141]. The F127, containing phenol/formalin/melamine as a reach source for N and C on pyrolysis resulted in the formation of N-doped carbon nanospheres (N-PCNs) revealed enzyme mimicking (POD, OD, SOD, and catalase activity (CAT)) activities up to four times/folds with intracellular ROS generation towards cancer therapy [142]. The MOF-based metalloenzymes, showed great catalytic potential along with doped carbon materials when combined with the moiety of M–N–C [143]. The Ca/Mg/Al modulated, nitrogen-doped graphene components developed *via* MOFs carbonization demonstrated a potent oxygen reduction tendency, better catalytic response in alkaline media, and a half-wave potential of 910 mV [144–146]. By using the precursor ZIF-8 MOF, Liu *et al*. developed a single-atom NZ of $Zn{-}N_4$ *via* single-step carbonization (at 800 °C under N_2 atmosphere)

[147] and exhibited the role of photosensitizer along with the response of POD-mimicking. Similarly, Fe–N_4 NZ was developed *via* carbonation (single-step) of ZIF-8 MOF at 900 °C (in the presence of iron phthalocyanine under nitrogen atmosphere) [148] and showed a brilliant SOD and CAT-mimicking responses for eliminating intracellular O_2 and H_2O_2 to preserve the cells from oxidative stress conditions. The development of Fe nanocatalyst (single atom) *via* carbonization of MOFs through PEGlyation exhibited exceptional Fenton reaction towards the elimination of overexpressing tumor cells [149].

3.2. MOF-derived carbon/metal oxide nanozymes

Apart from the developed NZ from M–N–C moiety, the NPs of metal oxide are having vast applications because of their low-cost synthetic procedures, flexible oxidation state, and greater ambient stability. Three different sizes of Fe_3O_4 NPs catalyze the oxidation of 3,3′,5,5′-tetramethylbenzidine (TMB) under the presence of H_2O_2 was reported by Yan *et al.* [150–152]. Nanourchins of $MoO_3{-}x$ with an elevated surface area, denoted potential therapeutic responses (PDT) through multiple enzyme cascades [153–157] Numerous mesoporous MOF-based derivatives were designed (*e.g.*, MOF modulated fluorescent carbon dots exhibiting exceptional fluorescent properties towards biosensing and bioimaging, silica-coated MOFs of $Mn_3[Co\text{-}(CN)_6]_2$ resulting an intrinsic CAT-mimicking catalytic response towards H_2O_2 (intracellular) followed by generation of O_2 endogenously) [158,159]. The thermally transformed crystalline cerium MOFs (CeO_2NPs) into fine form was encapsulated in meso–porous frameworks of n-CeO_2 NSs through one-pot facile calcination under N_2 atmosphere [160] revealed excellent oxidative damage followed by an induced energy depletion chemotherapy *via* adenosine triphosphate deprivation with minimum side effects. Huang *et al. via* low-temperature pyrolysis assisted solvothermal reaction (at Ar atmosphere) fabricated Co-mediated porous nanocages of C–CoM-HNC, where M stands for Mn, Ni, Zn and Cu [161] and revealed the tailoring of a better surface adsorption of energy (due to incorporation of Cu) followed by a d-band density in C–CoCu-HNC nanostructure resulting in mimicking of nanozyme and activates peroxymonosulfate towards elimination of organic pollutants [162].

3.3. Ferrum-based nanozymes

In today's era, the ferrum (Fe)-based NPs are widely recognized for numerous biomedical applications such as in CAT mimetic properties, POD mimetic activity, and magnetic resonance imaging (MRI) [163,164]. Mesoporous silica NPs encapsulated with Fe_3O_4 NPs and glucose oxidase (GOD) were found to be effective towards tumor catalytic response *via* the production of –OH [165–167]. As per the investigation of Gao *et al.* an increased proportion of Fe^{2+}/Fe^{3+} from Fe_3O_4 would be achieved while treated with $NaBH_4$, which helps in mimicking peroxidase-like activity whereas a reduced proportion of Fe^{2+}/Fe^{3+} (*via* $NaIO_4$ treatment) leads to reduction in POD-like response of Fe_3O_4 [168]. However, it has also been reported that the enzyme-like activity of the Fe_3O_4 could also be influenced *via* alteration in temperature, pH, and dimension of NPs. Wang *et al.* revealed that, in the physiological environment, the reducing agent (l-cysteine/NADPH) could be able to restore Fe^{2+} as well as Fe^{3+} on Fe_2O_3 surface potentiating the · generation –OH [169]. Chen *et al.* envied that, γ-Fe_2O_3 and Fe_3O_4 NPs at pH 4.8, exhibited better POD-like responses, whereas at pH 7.4, they exhibited CAT-like responses [170]. In tumor tissues, the overexpression of GSH leads to the reduction of Fe^{3+} to Fe^{2} and subsequent rise of the ROS level resulting destruction of tumor cells/tissues. With CAT-like response, Fe-based NZ (*e.g.*, development of Fe_3O_4 (Fenozyme) modulated recombinant human ferritin (HFn) with the capacity of crossing blood-brain barrier) are associated with ROS-based therapy of cerebral malaria in mice [171].

3.4. Molybdenum-based nanozymes

Molybdenum (Mo) NPs has also fascinated substantial courtesy as NZ [172–174] imparting catalytic mimicking activity as of CAT, OXD, SOD, and sulfite oxidase [175,176]. However, because of their constraints (carrying both oxidative and antioxidative activities) they are limited with their biomedical applications. MoO_3-x nanodots were synthesized by Han *et al.*, with SOD and CAT mimicking activities against Alzheimer's disease [177]. The pH-modulated multi-enzymatic activity-based MoO_3-x nanourchins (MoO_3-x NUs) were synthesized by Hu *et al.* for tumor therapy [178] revealed maximum biocompatibility (at physiological pH) because of the maximum stimuli-responsive biotransformation. Under acidic and high H_2O_2 conditions, MoO_3-x exhibited the best catalase activity to reduce the high concentration of Mo^{5+} atoms. MoO_3-x also demonstrated OXD-like response by converting H_2O_2 to O_2 endogenously, thereby resulting a better tumor-specificity by controlling the toxicity (acidic approach) of NZ.

3.5. Iridium-based nanozymes

Iridium (Ir) based NPs (NZ) showing CAT-like responses (*via* oxidation of metals) are widely applicable for their biomedical solicitations [179,180]. Su *et al.* revealed the formation of PVP-Ir NPs (upon the exposure of IrO_2 to H_2O_2) enabling CAT-like activity [181]. The electron transfer mediators demonstrated the generation of PVP-Ir NPs reporting POD like activities by preventing reactive nitrogen species (RNS) and ROS-mediated alleviation of acute kidney injury (AKI) [182]. Ir-oxide (IrOx) was also reported to possess pH-dependent CAT-like and acid-activated OXD like activities towards tumor targeting [183].

3.6. MOF-derived metal NPs/Carbon nanozymes

Because of the convenient synthetic procedure and facile post-synthetic surface alteration, metal NPs are excellent towards their role as sensors, detection, catalysis, and imaging. Rossi *et al.* unveiled the GOx-mimicking catalytic responses for the unaltered gold NPs [184]. Lin *et al.* reported that the catalytic efficacy of unmodified gold NPs was found to be maximum compared with the citrate-capped and amino-modified AuNPs towards oxidation of 2,2′-azinobis (3-ethylbenzothiazoline-6-sulfonic acid) (ABTS) and TMB [185]. In a different study, it has been observed that cysteine-adapted AuNPs unveiled POD-mimicking, whereas the citrate-modified AuNPs denoted GOx mimicking responses [186]. The growth of metal-conjugated M–N–C NZ, from a single-atom to a NPs scale, revealed the formation of another category of MOF, known as metallic composite/carbon or the metal/carbon hybrid with a more advanced catalytic efficacy [187]. MOFs *via* calcination get transformed into mesoporous carbon, forming metal nanocomposites with better catalytic and enzymatic activity. The CUNPs encapsulated within mesoporous carbon resulted in the formation of Cu-based MOFs. The resultant composites of Cu/C exhibited a higher H_2O_2 affinity with enhanced POD-mimicking responsiveness compared to the commercial horseradish peroxidase (HRP). A mesoporous carbon hybrid (N and Co co-doped) was synthesized by Huang *et al.*, with improved OD mimicking response towards the detection of glutathione (GSH) [188]. The ZIF-67 MOF *via* pyrolysis (one-pot) resulted in the formation of carbon nanomaterials and revealed an OD-impersonating response towards TMB, ABTS, and O-phenylenediamine (OPD) in the H_2O_2 absence [188,189]. Yoon *et al.* developed Cu@C-500 nanozyme (HKUST-1) from a Cu-modulated MOF. The GOx, in combination with Cu@C-500 explored

POD-mimicking catalytic response towards bio sensing of glucose [189].

3.7. MOF-based linker exchange strategy

Unlike several NZ (pristine derived MOFs), most of the MOFs showed enzyme-mimicking (intrinsic) responses based on their Lewis base and acid existing active sites. Numerous MOFs such as Zr-modulated UiO-MOFs (where UiO = University of Olso), Ni-modulated MOFs, Fe-based MIL-MOFs (MIL = Material Institute of Lavoisier), Prussian blue-based MOFs and Cu-modulated HKUST-MOFs (HKUST stands for Hong Kong University of Science and Technology) having POD-mimicking catalytic response were being fabricated [190]. MOFs like UiO-66 developed several novel derivatives with prismatic catalytic responses. UiO-66-NH_2 revealed a 20-fold increment in hydrolysis of phosphate-ester than that of UiO-66 MOF after organic linker exchange by amino groups [191]. The substitution of 2-methyl imidazolate (2-mim) *via* imidazolate in nBuOH of ZIF-8 system, exhibited a tremendous increment in Brønsted base catalytic response compared to the parent ZIF-8 MOF [192]. Similarly, Qu *et al.* generated PZIF67-AT NPs showing SOD-mimicking response to develop H_2O_2. The over-expressed H_2O_2 is further catalysed to form OH free radicals thus, stimulating Fenton reaction-modulated chemo dynamic therapy (*e.g.*, tumor suppression by PZIF67-AT nanozyme in the mice bearing Murine hepatoma tumor cells) [193].

3.8. MOF-based metal doping strategy

In contrast to the post-synthetic linker exchange, MOF derivatives resulted in the engineering of metal nodes exhibiting with enhanced enzyme-mimicking responses [194]. The development of metal nodes along with the organic linkers enhances the enzyme linked catalytic responses of the pristine MOFs towards a targeted approach for regulating the MOF-based derivatives [195]. The 2,2′-bipyridine-5,5′-dicarboxylic acid ligand bridged with Zr^{4+} and further altered with Cu^{2+} and bipyridine species resulted in the formation of UiO-based MOF NPs [196] and possess an enhanced catalytic response for oxidation of dopamine compared to Cu^{2+} alone as well as in combination with bipyridine. Similarly, Fe metal nodes binding with aliphatic diamines resulted in MIL-100(Fe), which could provogue the POD-linked catalytic functionalization of MOFs [197]. Besides transitional metal nodes, the noble metals could be associated with the development of MOF with better catalytic and/or enzyme-mimicking efficacy [198]. For regulating as well as anchoring electronic potentialities of single metal atoms, Wang *et al.* developed a series of synchronized single-atom metal sites (Cu, Co, and Au) by using Zr-modulated porphyrin MOF resonating nanotubes [199].

4. MOF-based nanozymes with their theranostic approaches

4.1. Biosensing

MOF-based NZ have been designed to develop sensors for the detection of several ions (H_2O_2) and biomolecules (macro and micro molecules) by implementing fluorescence, colorimetric, and electrochemical methods. Based on two constraints (detection ranges and limits) MOF-based NZ can be applicable as biosensors in an extreme concentration environment (for a wide detection range), and detection at specific regions with more accuracy (subjecting to a narrow detection range). The sensitivity of the biosensor was signified by its limit of detection [200].

4.1.1. Detection of biomolecules having the smaller size

MOF-based nanozymes are usually implemented for the detection of glucose thereby treating diabetes *via* monitoring the level of elevated blood sugar level *via* colorimetric detection technique. Zhao *et al.* reported that, the Fe(III)-BTC MOF resonated with glucose oxidase could also be useful in detecting the glucose within a 5–100 μmol/L level [201]. NiPd NPs and glucose oxidase immobilized on ZIF-8 showed a peroxidase-like activity and were useful in the rapid detection of glucose [202]. GOx@MOF-545(Fe) developed by Zhong *et al.* enabled glucose detection at 0.28 μmol/L, with maximum specificity and effectiveness (92%) [107]. Table 2 showing the summary of applications for several MOF-based nanozymes in detection of several components [200,203].

ZIF-67/TiO_2 doped with Cox Oy Hz nanotubes at a detection limit (0.03 μmol/L) and range (0.1 μmol/L to 1 mmol/L) was highly applicable for sensing a high concentration of glucose *via* fluorescence and colourimetric detection principles [204,205]. MOF-based nanozyme MIL-53(Fe) was useful in catalyzing glucose oxidation and H_2O_2 with terephthalic acid (TA) and was found to be sensitive for the detection of glucose [206]. The chemiluminescence efficiency (up to 35%) was achieved by a Cu^{2+} altered nano MOF (nMOF) in the presence of H_2O_2 and luminol [207]. A thorium-based MOF (Th-MOF) nanozyme detected the uric acid *via* the generation of H_2O_2 [208]. *Via* colorimetric analysis, Cu (PDA)-(DMF) MOF was able to detect salicylic acid [209], ascorbic acid [210], dopamine content [211] and thiamine [212]. NH_2–MIL-125(Ti) MOF added with Au is quite useful in the detection of photosensitive substances (hemicystine at the range of 1–10 μmol/L and value of 0.15 μmol/L) [213]. Valekar *et al.* applied MOF grafted with amine (TMBDA-MIL-100(Fe)) for fluorescence detection of acetylcholine and choline at a minimum detection value of 0.036 and 0.027 μmol/L, respectively [214,215]. A hybrid (cholesterol oxidase + MOF) reported a high catalytic activity and determined cholesterol (within a range of 0.06–15 μmol/L) at a detection limit of 0.03 mmol/L [216]. The Cu-MOF NPs developed by Wang *et al.* not only catalyze H_2O_2 but also helps in the detection of *Staphylococcus aureus* (at 50–10,000 CFU/mL) and within a limit of 20 CFU/mL [217]. Similarly, Fe-MOF NPs were used for the detection of *Salmonella enteritidis* at a detection value of 34 CFU/mL, and a recovery rate of 94.68%–124% (in milk) [218].

4.1.2. Ionic detection

MOF-modulated NZ are actively involved with ion detection in biological and environmental segments. PtNPs doped UiO-66-NH_2 NZ (mimicking peroxidase-like activity) were used for the adsorption of mercury ions and leads to remove Hg^+ ions from water (up to 99%) [219]. Ce-based MOFs (mixed valance) with oxidase-like activity made a complex when added to single-stranded DNA resulted in a high specificity towards the detection of Hg^+ (within a concentration of 0.05–6 μmol/L, along with the detection limit of 10.5 nmol/L). Moreover, the sensor revealed a better specificity towards the detection of Hg^+ [220]. ZIF/GO hybrid NZ are highly sensitive for the detection of Ag^+ in water and human serum (at a detection value of 1.43 nmol/L) [221,222].

4.1.3. Detection of biomacromolecules

The biological macromolecules such as proteins and nucleic acids were detected *via* MOF-based NZ. Wang *et al.* reported that the phosphorylated proteins were detected by a Zr based MOF (nanozyme) [223]. A Fe-MOF-GO-based nanozyme (with a detection limit of 0.268 ng/mL) was involved in biomarkers detection in human blood *via* exposure of wood smoke (benzo(a)pyrene diol epoxide (BPDE)-DNA) [224]. For thrombin detection in human serum, a colorimetric method was suggested by Wang *et al.* using an iron-mediated MOF (Fe-MIL-88A) aptamer with a very high specificity [225]. Li *et al.* carried out the detection of acid phosphatase (at a detection value of 0.005 U/L with a concentrations range within 0.01 U/L and 30 U/L) by using a MOF based catalyst (NH_2−MIL-101) by adapting the fluorescence detection technology

Table 2
Application summary of numerous MOF-based nanozymes in detection of components.

Materials ranges	Methods	Target detection	Limits (μmol/L)	Range (μmol/L)
Fe-MOF-GOx	Colorimetric	Glucose	0.487	1–500
Fe(III)-BTC	Colorimetric	Glucose	2.4	5–100
GOx@ZIF-8(NiPd)	Colorimetric	Glucose	9.2	10–300
GOx@MOF-545 (Fe)	Colorimetric	Glucose	0.28	0.5–100
Fe_3O_4/MIL-101(Fe)	Colorimetric	Glucose	0.0049	0.005–0.1
CoxOyHz@ZIF-67/TiO2	Colorimetric	Glucose	0.03	0.1–1000
MIL-53(Fe)	Fluorescence	Glucose	0.00844	0.5–27
Cu^{2+}-NMOFs	Fluorescence	Glucose	–	–
Th-MOF	Colorimetric	Uric acid	1.15	4.0–70
Cu (PDA)- (DMF)	Colorimetric	Dopamine	–	–
MIL-68 or MIL-100	Colorimetric	Ascorbic acid	6	30–485
HKUST-1	Fluorescence	Thiamine	1	4–700
Au@NH_2-MIL-125(Ti)	Fluorescence	Hemicystine	0.15	1–10
TMBDA-MIL-100(Fe)	Fluorescence	Choline	0.027	0.5–10
TMBDA-MIL-100(Fe)	Fluorescence	Acetylcholine	0.036	0.1–10
MIL-101(Fe)	Fluorescence	Choline	0.02	0.1–10
MIL-101(Fe)	Fluorescence	Acetylcholine	0.008	0.01–100
ChOx-MOF	Fluorescence	Cholesterol	0.03	0.06–15
Pt NP@UiO-66-NH_2	Colorimetric	Hg^+	0.00035	0–0.01
Ce-MOF	Colorimetric	Hg^+	0.0105	0.05–6
ZIF/ GO	Colorimetric	Ag^+	0.00143	0.002–0.005
Zr-MOF	Colorimetric	Phosphorylated proteins	–	–
MOF@Pt@MOF	Electrochemical	Exosomal miRNAs	2.9×10^{-10}	10^{-9}–10^{-3}

[226]. MOF-based bimetallic hollow nanocages (revealed oxidase-like activity) with their metal doping and hierarchical structure provides adequate numbers of active sites for the detection of acetylcholinesterase within a range of 0.0001 mU/mL to 1 mU/mL and under a detection limit of 0.1 mU/mL [103]. MOF-based NZ are also engaged with the bio-sensing of several enzymes like deoxyribonuclease and phosphatase [227–229]. MIL-88@Pt@MIL-88, a multiple-layered nanozyme material *via* electrical signal transduction used for detection of exosomal micro RNA (miRNA), as a tumor biomarker [230]. Sun *et al.* developed a Fe_3O_4 (Fe_3O_4@UIO-66/Cu@Au and Cu@Au modified magnetic nanozyme combined with DNA nanotetrahedron towards the detection of cardiac troponin I (a biomarker of myocardial infarction) *via* electrical signal transduction, maintaining a detection range of 0.05–100 ng/mL and detection limit of 16 pg/mL [231]. Ling *et al.* developed a NZ altered with platinum NPs (Pt@P-MOF(Fe), used as a carrier towards an assistant DNA strand (aDNA1) for the bio sensing of telomerase along with the measurement of the concentration of HeLa cells [232–237].

4.2. Cancer therapy

In today's ear, cancer is considered a prime health issue around the globe, caused by a malignancy associated with solid tumors. Despite the availability of multiple traditional therapeutic approaches, the major concern includes low selectivity and substantial side effects. To overcome/minimize the complicacy of traditional therapeutic approaches, several novel slants such as starvation therapy, photodynamic therapy (PDT), chemo dynamic therapy (CDT), photothermal therapy (PTT), immunotherapy as well their combination has been implemented [238]. MOF-based NZ are one of the exciting approaches towards tumor therapy signified by adaptable chemical composition, varied catalytic structures and virtuous biocompatibility [239]. The anti-tumor potential of MOF-modified NZ is governed by the development/generation of $^1O_2$, HClO, –OH, ROS, H_2O_2 and O_2. The surface of the nanomaterials modulated *via* appropriate ligands or antibodies can leads to enriching them into the specific organs/cells within the body, *e.g.*, targeting of triple-negative breast tumors *via* Zr-UiO-66 functionalized pyrene-derived polyethylene glycol (Py−PGA-PEG) conjugated with (F_3)-nucleolin ligand [240]. Zr-UiO-66 revealed a strong material as well as radiochemical stability throughout several biological media. Based on PET and cellular targeting analysis, it was observed that Zr-UiO-66/Py−PGA-PEG-F_3 could be an image-guided, nano platform towards the delivery of tumor-selective cargo [241–243].

Many anticancer drug moieties were targeted into the tumor sites based on their passive enhanced permeation and retention (EPR) effect. Passive targeting of PCN-224 was varied with respect to the particle size of the nanoconjugates [244]. The TCPP@PCN-24 revealed a best photodynamic therapy response at a particle size of 90 nm and worst response at 190 nm. The MOF of AZIF-8 exhibited better anti-tumor response at 60 nm because of strongest retention at tumor site [245]. MOFs associated with specific ligands like RGD peptide, folate, and aptamers *via* monoclonal antibodies converted into immune microspheres and inhibited by the macrophage uptake, thus targeted into the carcinoma cells for exploring theranostic potentials [244]. Li *et al.* developed FA/DOX@UiO-68 [246] and IRMOF-3@CCM@FA (for curcumin delivery into triple negative breast cancer cells) and confirmed the tumor targeting of the nanosystem *via* the responses of an internal/external stimuli [247–250].

4.2.1. Chemo dynamic therapy

CDT is a smart approach towards cancer therapy in which the elevated concentration of ROS was garnered for apoptosis of tumor cells (*via* Fenton reaction/generation of –OH ions from catalysis of H_2O_2) with reduced side effects and apparent selectivity. However, there is an issue of insufficiency of cellular H_2O_2. In order to correct the deficiency of H_2O_2 (regulation of Fenton reaction), Fang *et al.* developed glucose oxidase-loaded Co-ferrocene MOF to increase the concentration of -OH radicals for maximizing CDT effect [251]. Tian *et al.* have developed the MOF of Ce-benzenetricarboxylic acid encapsulated with lactate oxidase for enhancing the cellular level of H_2O_2 *via* increment in ROS production for apoptosis onco cells [252]. Later on Li *et al.* designed a cascade of Fe- ZIF-8 magnetic MOF NPs encapsulated with glucose oxidase towards cancer CDT [87]. Ding *et al.* prepared gold NPs loaded MOF for an effective CDT of cancer with an extended time of retention [97]. Aluminum-carbide modulated MOFs lead to derive graphite NZ by Jun *et al.* was successfully targeted for tumor CDT at a reduced pH condition [253]. Burachaloo *et al.* designed Iron-based

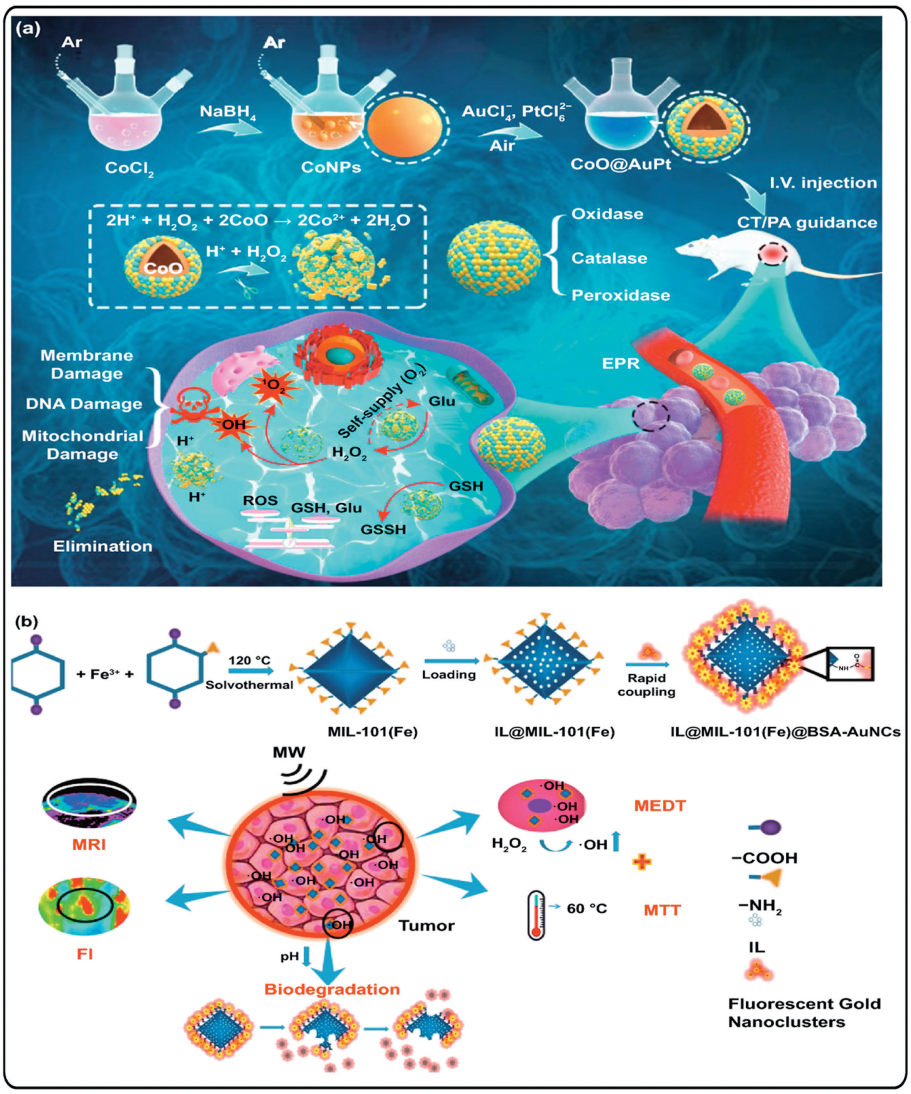

Fig. 1. (a) Preparation and the catalytic mechanism for CDT enhancement of CoO@AuPt NPs *via* Fenton reactions and regulating the response environment. (b) Preparation, degradation process and the therapy principle of IL@MIL-101(Fe)@BSA-AuNCs NPs for MEDT. GSSH Glutathione disulfide, EPR enhanced permeation and retention, MW microwave, MRI magnetic resonance imaging, MTT microwave thermal therapy, FI fluorescence imaging. Reproduced with permission [222]. Copyright 2021, Springer.

MOF to enhance the concentration of free radicals of –OH, thereby applied for CDT-oriented cancer cell apoptosis assorting minimum harm towards the healthy cells/tissues [254]. Zhang *et al.* proposed imidazole-based MOF (ZIF-8) NZ embedded with glucose oxidase and chlorperoxidase. The outcome of the study revealed that the developed nanozyme exhibited a seven fold increase in the clearance of tumor cells compared to the normal neutrophils [255]. Fig. 1 shows the synthesis and catalytic impact for CDT augmentation of CoO@AuPt NPs through Fenton reactions, regulation of synthesis, biotransformation and applicability of IL@MIL-101(Fe)@BSA-AuNCs NPs towards EPR modulated permeation enhancement, magnetic resonance imaging (MRI) and microwave thermal therapy (MTT) and fluorescence imaging (FI) [222].

4.2.2. Metal doped MOFs modulated photodynamic and photothermal therapy

PDT is usually showing its anticancer potentiality *via* photosensitization (PS) of drugs followed by laser activation. The building of drug concentration in tumor tissues, leads to elicit photochemical reaction (development of cytotoxicity *via* activation of singlet oxygen ($^1O_2$) thereby damaging the tumor tissues [256–258]. The fluorescence tendency of the photosensitizers (ROS activation leads to DNA damage and causes tumorigenesis) help in generating an upgraded temporal, spatial and safe imaging towards tumor therapy [259–265]. Zr-based MOF (UIO-PDT) is considered to be a superb PDT reagent and imparted its anti-cancer response *via* solvent-assisted ligand exchange process (by stimulating photo generated ROS production) [266]. PDT is an exciting approach for cancer therapy, which regulates the formation of reactive $^1O_2$ *via* ROS production by using the principle of photosensitizer (PS) [239]. However, the occurrence of unusual hypoxia not only affects the metastasis and growth of cancer cells [267] but also causes serious hindrances towards the efficacy of PDT. To overwhelming such issues, different MOF-based NZ were reported for the smooth functioning of PDT. The 5,10,15,20-tetra(pbenzoato) porphyrin (TBP)-modulated MOFs (TBP-MOFs) and the platinum NPs based MOFs, denoted apoptosis of cancer cells by formation of $^1O_2$ and resulting catalase-like response along with better stability and effective in PDT [268,269]. Lan *et al.* designed mesoporous MOF NPs, that induce TBP-MOFs for PDT with a curing rate of around 60% along with 98% of tumor reduction capability [270]. Wang *et al.* developed Ru-modified $Mn_3[Co(CN)_6]_2$ MOF containing chlorin e6 (Ce6) in order to nullify

the issue of hypoxia in tumor microenvironment. The developed MOF denoted an effective biocompatibility with an efficient loading capacity for Ce6 [271,272]. Researchers developed Au mediated Fe-based MOFs NPs [273], Au-doped MOF NPs (Au@ZIF-8) [274], ZIF-8 based MOF incorporated with Al(III) phthalocyanine chlorotetrasulfonic acid [275], Cu-MOF $\{CuL\text{-}[AlOH]_2\}_n$, porphyrinyl-MOF and $MnFe_2O_4$@MOF modulated NZ (by reducing/adsorbing concentration of GSH) [276–279], resulting a cascade of anti-tumor responses by overwhelming the PDT oriented issues [274].

In PTT, the materials injected have higher photo thermal conversion tendency (irradiation) near the tumor tissues *via* targeted recognition principle at interior parts of human body [280]. The PTT of several types include organic/inorganic photo thermal converters (*e.g.*, gold nano plates and poly dopamine particles) [281–284]. The immunological mechanism associated with PTT revealed the photo thermal immunotherapy governed by organic semiconducting polymer nano adjuvant ($SPN_{II}R$) associated with laser irradiation in presence of second infrared window (NIR-II) causing tumor cells death *via* ablation of hyperthermia (release of R848 in tumor cells) and elevated consumption of glutathione [285,286]. The antitumor response *via* immunotherapy can be modulated *via* stimulating the immunity of the human body, inhibiting the immune checkpoints, deployment of cancer vaccines and therapeutic antibodies [287,288]. However, the approaches like programmed cell death ligand 1 (PD-L1) and cytotoxic T cell-associated antigen-4, programmed cell death receptor 1 (PD-1) were recognised and approved by US Food and Drug Administration (FDA) as the potential approaches (immune checkpoint inhibitors) against breast cancer. The development of MOFs like Fe-CPND and Zr-Fc MOF showed a higher PTT. However, the PTT response of Fe-CPND was because of the LMCT effect, which is due to the existence of Fe–phenol structure [266,289–291]. The MOF modified with AS1411 aptamer, and polyethene glycol denoted better stability, and target orientation towards tumor cells without affecting the viability for healthy cells [127,292,293].

Metal-doped MOF loaded with Photo thermal agents (PTAs) (*e.g.*, AuNPs) endowing with multivalent approaches like chemo-photo thermal therapy, fluorescence imaging, and controlled drug delivery [294,295]. Zr@PDI and Zr-PDI were successfully used in boosting up of NIR towards the photo thermal conversion of perylenediimides against cancer therapy and photocatalytic reactions. [296–316]. However, polymer-coated MOF denoted high specific surface area with more footholds, could be highly effective towards PTT based cancer therapy. The MOFs of polymeric elements such as polypyrrole (PPy), polydopamine (PDA) are being recognised as excellent photo thermal transducer along with good biocompatibility, stability, and degradation tendency. Thus, such elements with utmost photo thermal efficiency are being explored for cancer irradiation *via* chemo-photo thermal therapy. Polypyrrole-coated MOF linked with azo benzene tetra carboxylic acid (H4-ABTC) is a potential asset for PTT mediated tumor therapy [317,318]. PPy-coated Fe-soc-MOF (Fe-soc-MOF@PPy) is another multifunctional theranostic element showing elevated photo thermal conversion efficiency with a better NIR 808 nm adsorption tendency [319,320]. Polydopamine-coated MOFs like UIO-66, DOX@ZIF-8, ZIF-8, PDA@ZIF-8 and MIL-101 are widely engaged in PTT and PDA [321–323].

4.2.3. Targeted starvation

This therapeutic approach is associated with inhibiting access of glucose to the tumor cells (starvation therapy) thereby inducing scarcity for supply of energy, leading to cell lysis [40]. The erythrocyte-membrane wrapped MOFs encapsulated with glucose oxidase and tirapazamine (TGZ@eM) acted as a nanoreactor, (by reducing the glucose level and inducing O_2 demand), leading to restricting the energy supply and causing hypoxia and death in tumor cell. The approach was showing a positive response toward colon cancer [324]. Li *et al*. designed glucose oxidase and catalase-embedded MOF for a combined PDT and starvation therapy (*via* the formation of $^1O_2$ and reduction of glucose supply) [325]. Similarly, by adapting the above principle, Liu *et al*. developed catalase-like Pt NPs loaded over porphyrin-based MOF for tumor targeting [326]. Fig. 2 presented the schematic illustration for the synthetic route of PCP-Mn-DTA@GOx@1-MT nanozyme towards their combined applications in oxidation, starvation, and immunotherapy [327].

4.2.4. Immunotherapy

The induction of immune system in human body causes lysis of several carcinoma cells *via* immunotherapy. The approach leads to minimizing tumor metastasis and recurrence. Despite of poor response of immune-based cancer therapy, MOF-based NZ are highly adaptable to immunotherapy for turning out the trend [328]. Lan *et al*. developed MOF (Fe-TBP) based nanozyme "tumor vaccine" for PDT-induced generation of $^1O_2$ in a hypoxic environment to develop an anti-tumor effect [329]. Such material was found to be effective against colon cancer (with a tumor curing rate of 90%) in mice models [330]. Immunotherapy *via* checkpoint blockade (by blocking the pathway for T-cells targeting) is a very popular concept in cancer therapy. Ni *et al*. designed a MOF-derived combination therapy (immune checkpoint blocking + radiotherapy). The outcome of the study revealed a 50% curing rate after 10 sequential therapy with exposure of X-rays and the HF12-DBA MOF in the mouse model [331]. By combining checkpoint-blocking immunotherapy, CDT, and PDT, Ni *et al*. developed Cu-porphyrin nMOF. By following the cascade of ROS/$^1O_2$ induction principle, the method has obtained a positive response of around 33.3% towards curing of cancer in a mouse model [332].

4.2.5. Other cancer therapies

MOF-based NZ are also associated with several miscellaneous treatment options such as, microwave thermotherapy, microwave dynamic therapy, and sono-dynamic therapy. Fu *et al*. reported the use of Mn-ZrMOF nanocubes in combination of microwave thermotherapy and microwave dynamic therapy for the treatment of cancer [114]. The iron-based MOF nanozyme (MIL-101(Fe)) induced death of cancer cells (up to 96%) by catalyzing the formation of -OH in large amounts under microwave irradiation (microwave dynamic therapy) [333]. MOF-derived carbon nanostructure on exposure to ultrasound generates huge concentrations of ROS, which results in inhibition of tumors *via* sono-dynamic therapy (success rate up to 85%) [86].

4.2.6. Combination therapy

The combination of PDT and starvation therapy [325,326] as well as the combination of PDT and CDT with immunotherapy [330,332] showed better efficacy in tumor targeting. The ultrathin Zr-FC MOF nanosheets were showing synergistic impact with PTT and CDT; resulting a higher photothermal conversion rate (up to 53%) in both *in vivo* as well as *in vitro* studies [334]. Fig. 3 unveiled the working principle of TiO_{1+x} NRs and $PtCu_3$-PEG nano cages towards combined SDT/CDT-tumor therapy [222].

4.3. Theranostic impact on diabetes

In 21st century Diabetes, could be considered as the disease of the millennium causing a major conspiracy towards the human body [335,336]. MOFs are quite a few attracted towards the detection of acetone in the breath of diabetic patients (usually found to be more than 1.8 ppm in diabetic compared to 0.3–0.9 ppm in normal human beings) based on their greater porosities and surface area [337,338]. Chang *et al*. developed a ZnO@MoS_2 MOF

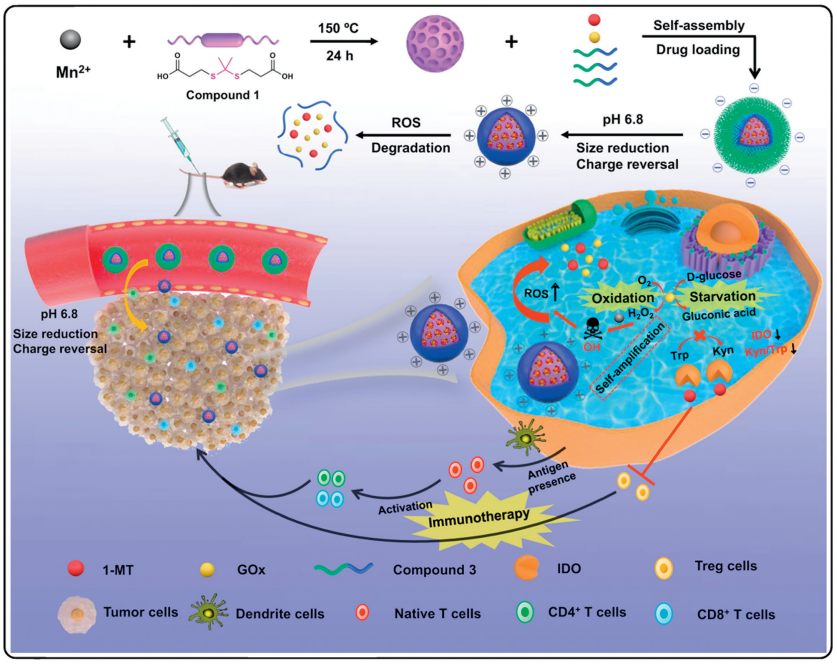

Fig. 2. Synthetic route and schematic illustration of PCP-Mn-DTA@GOx@1-MT nanosystem for combined starvation, oxidation and immunotherapy. Reproduced with permission [327]. Copyright 2022, Nature.

nanosheets for the detection of acetone. The outcome of the report revealed an ultra-fast detection of acetone (60 s/40 s @5 ppb and 9 s/17 s@ 500 ppb) because of the faster diffusion of acetone *via* the mesoporous MoS_2 nanosheets [336]. Similarly, Gutiérrez *et al.* transformed MOFs of non-luminescent type (OX-1 (Zn-BDC)) into the faster luminescent MOFs (OX-2 (Ag-BDC)) for the development of fluorometric sensors for a faster theranostics of diabetes analyzing the acetone concentration [339]. Such techniques are governed by better stability, lesser detection limits, and a lesser environmental reliance [340]. Wang *et al.* explored their research for developing a nickel/cobalt-based nanohybrid MOF (NiCo-MOF) for systemic detection of glucose within a detection limit of 0.05 μmol/L to 4.38 mmol/L, under an optimized voltage (0.50 V) [335]. In another study, Wei *et al.* developed a modified, portable MOF nanozyme of cobalt/carbon cloth/paper (Co-MOF/CC/Paper) for glucose detection of in saliva, serum, and urine samples and revealed better stability, durability, selectivity, along with exceptional robustness [341].

Since for a long time, the world has already been engaged in the mission of developing non-invasive oral insulin therapy, but unfortunately not that much lucky to get a solution yet, despite of few revolutionary trials by the pharma giants. One of the biggest hurdles for such a delivery system is the stability issue of insulin in the gastric pH condition (pH 1.5–3.5). However, MOFs with adequate modifications are being tried for a nasty challenge to deliver encapsulated insulin in oral route [342]. Chen *et al.* encapsulated insulin in zirconium-based MOF, (NU-1000) and unveiled the stability of insulin in gastric pH and enzyme system followed by a sustained release action [342]. Zhou *et al.* designed microspheres (Ins@MIL100/SDS@MS) loaded with NPs of sodium dodecyl sulphate modulated iron-based MOF (MIL-100) for delivery of insulin *via* oral route [343]. Microspheres (under acidic pH), revealed a sustainable degradation with a better bioavailability compared to the raw insulin. A glucose-responsive nano-carrier system (ZIF@Ins&GOx) loaded with glucose oxidase and insulin was developed by Zhang *et al.* using ZIF-8 nanocrystals. The developed MOF-encapsulated insulin was protected from its degradation and maintained the systemic glucose level over a prolonged period (*i.e.*, 72 h) [344].

4.4. Wound healing

Chronic wounds, specifically diabetic foot ulcers (DFUs) are conceded to be the emerging challenges in the forefront of the physicians, making the healthcare expenses very high [345–347]. The Cu^{++} based MOF NPs (HKUST-1 NPs) incorporated into poly-(poly ethylene glycol citrate-*co*-*N*-isopropyl acrylamide (PPCN) hydrogel exhibited wound healing (followed by deposition of collagen, angiogenesis, and re-epithelialization) with a sustained release for Cu^{2+} along with reduced apoptosis and cytotoxicity [345]. In a similar way, Xiao *et al.* designed folic-acid-altered HKUST-1 (F-HKUST-1) MOF for diabetic wound healing [346]. Zhang *et al.* synthesized nitric oxide (NO) loaded HKUST-1 copper MOF for diabetic wound healing *via* electrospinning method [347]. The release of Cu and NO leads to the complete healing of diabetic wounds within four weeks [347]. Recently, Li *et al.* developed (dimethyloxalylglycine (DMOG)) loaded cobalt-based MOF (ZIF-67) for accelerating diabetic wound healing. The DMOG loaded ZIF-67 nano-fibrous scaffold (PLLA/gelatin) showed a prolonged drug release pattern (up to 15 days) followed by angiogenesis, sustainable collagen deposition, and inflammatory diminution at the target site [348]. MOFs based single-atom catalysts (SACs), are nowadays strongly engaged with wound healing. Zinc-carbon derived MOF (ZIF-8) containing zinc atoms demonstrated wound healing activity without causing considerable toxicity towards multiple organs/tissues system [349].

4.5. Neurological diseases

Neurological diseases specifically associated with the brain and spinal cord are most often associated with the disorientation of inflammatory network and oxidative stress and mostly originated either from hereditary genetic deviations or ageing or impaired glutathione (GSH) level (deviated from 0.5 mmol/L to 10 mmol/L) or issues with the immune system [350] Causing neurological disorders like Alzheimer's disease, autism, and schizophrenia [351]. Zhu *et al.* discovered MOF-based (Eu^{3+}/Cu^{2+}@ UiO-67-bpydc) fluorescence probe, for GSH detection in human serum. An increased

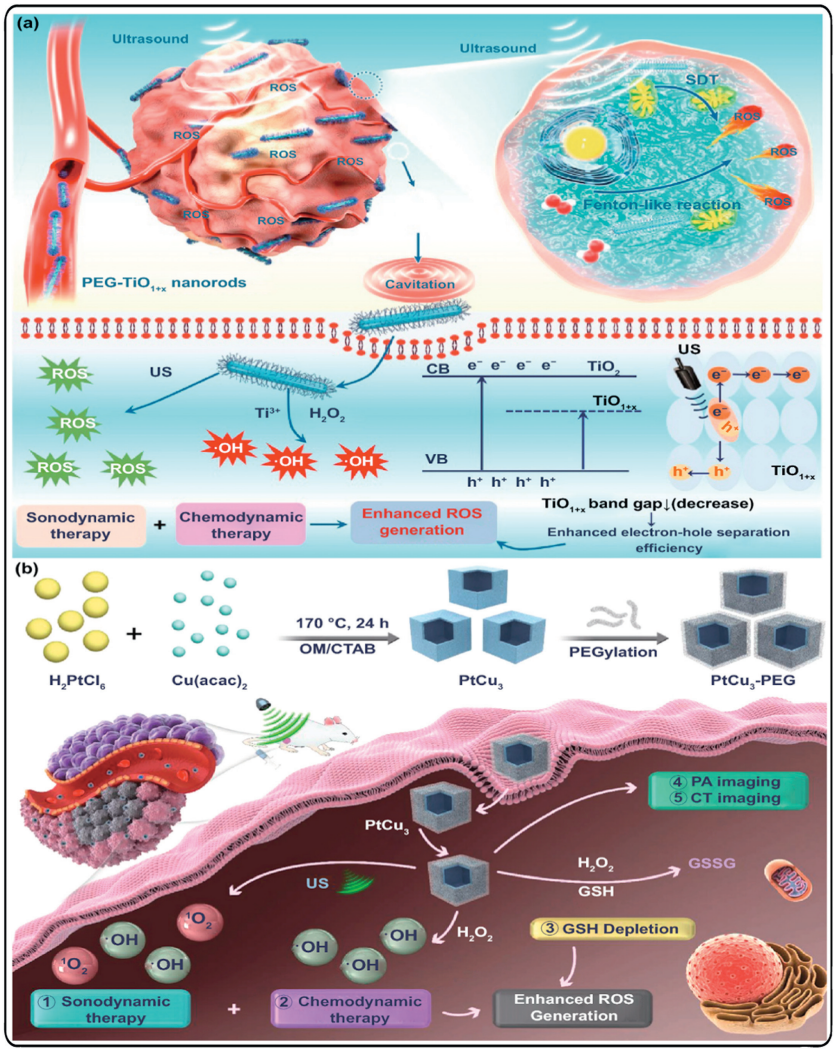

Fig. 3. (a) Schematic illustration of the working mechanism of TiO_{1+x} NRs with HRP-like activity for SDT/CDT-combined tumor therapy. (b) Preparation procedure and working mechanism of $PtCu_3$-PEG nanocages with HRP- and GPx-type property for PA/CT dual-modal imaging-guided CDT-enhanced SDT. Reproduced with permission [222]. Copyright 2021, Springer.

fluorescence intensity of the probe leads to the detection of GSH [352]. Chen *et al.* [351] developed P-DNA@MOF, [a 3D MOF for {[Cu(Cdcbp)(bipy)]$_4$H$_2$O}n loaded by means of FAM-labeled T-rich PDNA] for dual-sensing of for detection of Hg^{2+} and GSH useful in the diagnosis of neurodegenerative disorders. Alzheimer's disease (AD) is a crucial neurodegenerative disorder usually affecting the elderly population (above 65 yrs); manifested by memory loss, gradual declinement of cognitive capacity followed by functional impairment and causes global dementia [353,354]. The presence of metal ions (Fe^{3+}, Cu^{2+}, Zn^{2+}, and Al^{3+}) in brain (more than 3–7 times of a normal human being) is found be a crucial cause for the development of AD 3–7 times [354]. MOFs based derivatives (biosensors) are not only associated with the diagnosis but also treatment of Alzheimer's disease (AD) [353,354]. Fe-MIL88B-NH_2-NOTA-DMK6240 MOF loaded with Methylene blue (inhibits tau aggregation followed by decomposition of tau fibril) was synthesized towards the theranostic purpose of AD [355]. Wang *et al.* recommended synthesis of Porphyrinic Zr MOF (PCN-224) NPs for suppression of Aβ aggregation (*via* NIR-light-tempted inhibition of Aβ towards the formation of β-sheet) for treatment of AD. The results denoted that, PCN-224 NPs reduced the Aβ aggregation along with the cytotoxicity towards PC12 cells [356].

4.6. Ocular diseases

The drug delivery for treating the diseases like macular degeneration, glaucoma, and blepharitis are one of the most challenging task, because the majority of the administered drugs are unavailable into the target sites (only 5% of the administered drugs find their way to intraocular tissues) [357]. MOFs are being appraised to be the most exciting nanocarriers for ocular drug delivery of drugs [357,358].

4.7. Lung diseases

The lung disease like COPD (chronic obstructive pulmonary disease), asthma, ALI (acute lung injury), and fibrosis are some of the very common as well as life-threatening diseases which found to be more eye-catching during these days [359]. Hydrogen sulphide (H_2S) is considered to be one of the finest biomarker for the detection of asthma. MOFs seem to be providing a sensational platform for H_2S detection (fluorescent composite (Eu^{3+}/Ag^{+}@UiO-66-$(COOH)_2$) MOF detected H_2S in blood serum to confirm asthma) in the biological samples with a detection limit of 23.53 μmol/L [360]. Zhu *et al.* developed bimetallic MOFs (FexAl1-x-MIL) for detection

of H_2S and eosinophilia with a detection limit of 0–38.46 μmol/L [361]. Wang *et al*. established an MOF (fluorescent Zn(II)-based) for the treatment of asthma in childhood. The diminution in inflammatory retort recognised the MOF as a promising moiety towards the treatment of asthma in childhood [359]. By augmenting the principle of dry powder inhalers (DPI) Li *et al*. developed MOF particles of cyclodextrin (CD-MOFs) loaded with Paeonol for treatment of acute lung infections. The evaluation results of the drug-loaded DPI denoted promising responses (*in vivo*/*in vitro*) compared to the original drug candidate [362]. Similarly, theophylline-loaded Fe-MIL-100 was developed by Strzempek *et al*. against asthma and COPD [363]. The results confirmed the supremacy of MOF to be implemented for inhalational therapy [363].

4.8. Viral infections

With the advent of novel sensing technology, MOF-derived biosensors are widely applied for the detection of several viruses such as COVID-19, Zika, Ebola, influenza, acquired immunodeficiency syndrome (AIDS), and rabies [364,365]. Qiu *et al*. [366] investigated on 3D Cu(II)-modulated MOF of $\{[Cu(Cmdcp)(phen)(H_2O)]_2\text{-}9H_2O\}_n$ loaded with P-DNA to design a fluorescent sensor for a simultaneous detection of Ebolavirus-encrypted micro RNA-like fragment (miRNA-like) and Ebolavirus. The sensitivity recorded towards the detection of RNAs was mind-blowing with a peculiar limit of detection (60 pmol/L for miRNA-like Ebola virus and 206 pmol/L for Ebola virus). Similarly, Qin *et al*. explored a 3D dysprosium (Dy) MOF $\{[Dy(Cmdcp)(H_2O)_3](NO_3)\_2H_2O\}_n$ for revealing Ebolavirus RNA. The outcome showed a high sensitivity as well as selectivity towards the Ebolavirus RNA with a limit of detection at 160 pmol/L [367]. By implementing an electrochemiluminescence (ECL) RNA sensing platform (ultrasensitive switchable type), Zhang *et al*. developed Fe-MIL-88 MOFs based MOG (metal-organic gel) for the detection of Zika virus. The sensor unveiled great stability, specificity, and best sample detection capacity [368]. Xie *et al*. reported a 3D Cu-modified MOF $[Cu(Dcbcp)(bpe)]_n$ for concurrent detection of RNA sequences in Zika and Dengue virus. The efficiency of detection was found to be very sound and could be enhanced with the addition of SFA (synchronous fluorescence analysis) by improving the limits of detection [369]. The molecular imprinted polymers (MIPs) impregnated with magnetically fluorescent (MIL-101-NH_2) MOF were developed for the detection of hepatitis A virus. The MOF exhibited excellent sensitivity and selectivity for MIP sensors [370]. Yang *et al*. investigated on MIL-101@SiO2 NPs, for the detection of JEV (Japanese encephalitis virus) in serum samples. The sensor exhibited a satisfactory response towards the detection of the virus [371]. Marcos-Almaraz *et al*. developed an iron(III) trimesate MIL-100(Fe) nano MOF encapsulated with lamivudine triphosphate (3TC-Tp) and azidothymidine triphosphate (AZT-Tp) for advancing anti-HIV therapies [372].

4.9. Anti-bacterial activity and ROS scavenging

H_2O_2 is considered to be a very good weapon against numerous pathogenic microbiota. Nevertheless, the concentration of excess H_2O_2 leads to impart damage to the fresh tissues, but still is not considered as a part of wound healing. In order to overcome such issues, peroxidase-mimicking NZ have been introduced to such areas of research [77]. The ultra-small Au/MOFs were developed by combining ultrathin 2D MOFs to gold NPs, which revealed an antibacterial effect by removing *Staphylococcus aureus* (81.98%) and *Escherichia coli*, and resulting in wound healing [373]. The Fe modulated MOF NPs (MIL-100(Fe)) embedded with fluorescent 3-azido-D-alanine, catalyses the generation of O_2 from H_2O_2 enabling the development of ROS ($^1O_2$) resulting in the anti-bacterial responses (up to 75%) [374]. Zhang *et al*. developed a photosensitive MOF containing Ag^+ ion externally coated with hyaluronic acid (HA). The release of Ag^+, was governed by degradation of HA *via* bacterial hyaluronidase, leads to catalyse the formation of ROS and thereby shows anti-bacterial/wound healing responses [375–377]. To increase the anti-bacterial/antibiotic potential of the NZ, an injection was proposed (MOF-based NZ containing a small amount of Ag^+ solution) to develop NH_2_MIL-88B(Fe)-Ag, which revealed a very good antibacterial response against *E. coli* along with a reduced dependency on the concentration of H_2O_2 [378]. Zhuang *et al*. designed Co-MOF NZ, which denoted anti-bacterial response (*via* rupture of the bacterial cell membrane) through catalysis of the lipid oxidation with 100% recyclability and a durability of 4 weeks at an optimized pH range between 3 and 4 [379]. The above pH-related issue was overcome by using ultrathin 2D MOF (2D Cu-TCPP(Fe)), which maintains the pH between 3 and 4 (by reducing it from the neutral region) through catalysis of gluconic acid *via* glucose oxidase, thus resulting an establishment of pH-independent antibacterial responses [380]. The MOF based nanozymes and their biomedical applications were specified in Table 3 [381,382].

The antibacterial responses are often governed through the generation of ROS (H_2O_2, dO_2, and OH) [383–385]. CAT, SOD, and GPx are utilized for maintenance of the oxidative stress in cells. SOD leads to the conversion of dO_2 into H_2O_2 and O_2. Similarly, CAT and GPx catalyzed the developed H_2O_2 into O_2 and H_2O. The production ROS in excess damage the proteins, DNA, and lipids fragments of the biomolecules, associated with different disease conditions such as diabetes, cancer, cardiovascular disease, aging and neurodegeneration [386,387]. Mn_3O_4 nanozyme (nano flower) developed by Mugesh *et al*., exhibited GPx, CAT, and SOD like activities much better than conventional ones [388]. Ma *et al*. synthesized a Nitrogen-doped mesoporous carbon (FeSAs/NC) *via* pyrolysis of Fe-Pc@ZIF-8 precursor in N_2 atmosphere which exerted SOD-like activity and helps in catalysis of dO_2 to H_2O_2 and O_2. Further, the elimination of H_2O_2 and dO_2 from the intracellular level leads to protect HeLa cells from oxidative stress. By using pyrolysis at high temperatures, Cao *et al*. synthesized Co-doped ZIF-8. The developed MOF eliminated dO_2 and H_2O_2 through a cascade of CAT-mimicking, SOD-mimicking, and GPx-mimicking reactions [389].

4.10. Anti-inflammatory activity

ROS are considered to be the intermediate products obtained through cellular metabolism, which are going to be prevented/neutralized *via* the implementation of numerous antioxidants. However, on exceeding the production of ROS beyond the capacity of cellular antioxidant scavenging, it leads to accumulation and generates inflammatory retorts [390]. Prussian blue NPs provogues their anti-inflammatory responses by removing ROS *via* simulation of the activities of superoxide dismutase, peroxidases, catalases, and certain other enzymes [130]. Similarly, polypyrrolidone modified Prussian blue NPs are useful in reducing colitis in mice [391]. A Mn-TCPP-doped MOF scavenges ROS *via* simulating catalase and superoxide dismutase, thereby applied for treatment of ulcerative colitis and Crohn's disease [392,393].

4.11. Gene therapy

With a proper regulation/expression of genes, personalized therapy towards numerous diseases, is nowadays gaining prior attention. MOFs are not only being considered as a sound carrier for Cas9/sgRNA compounds, small interfering RNA (siRNA), and plasmids but also targeting ZIF-8 coated platelet cell membrane (as a platform for siRNA delivery) for effective gene silencing, and tumor targeting [394]. Similarly, pooled siRNAs (VEGF siRNA + *P*-gp siRNA) loaded over the surface of modified MIL-101(Fe) (sele-

Table 3
MOF based nanozymes and their biomedical applications.

MOF	Carrying drugs/Enzymes	Applications
Fe-MIL-101-NH_2	Isoniazid	Used as a theranostic towards Tuberculosis. The drug loaded MOF revealed a continuous drug release.
MOF-53 (Fe) NPs	Vancomycin (Van)	Improved drug loading capacity (20 wt%), antibacterial response of 99.3%, better biocompatibility and stability in acidic environment.
MIL-100 (Fe) NPs	3-Azido-D-alanine (D-AzAla)	Revealed a Faster accumulation and degradation after intravenous injection. Also denoted with integration specificity of d-AzAla with bacterial cell wall.
Fe_3O_4@PAA@ZIF-8	Ciprofloxacin (CIP)	Showing an upended drug loading (93%) and drug release (73%) capacity followed by an enhanced bacterial growth inhibition.
ZIFs	Cytochrome c, horseradish peroxidase, lipase, *etc.*	Bio-sensing
ZIFs	Catalase	Bio-sensing
ZIF-8	Lipase, β-galactosidase, glucose oxidase, *etc.*	Bio-sensing
ZIF-8	Glucose oxidase, horseradish peroxidase	Proof of concept, bio-catalysis
La/Fe/Zr-MOF	Acetylcholinesterase	Bio-sensing
UiO-66, MIL-53	Lipas	Synthesis of Warfarin
Cu-MOF, ZIFs	Trypsin, tyrosinase	Bio-sensing
IRMOF-3	Protein, lipase	Transesterification
PCN-888	Horseradish peroxidase, Glucose oxidase	Proof of concept
Tb-TATB	Cytochrome c	Mechanism comprehension
UiO-66-NH_2	Hydrolase	Asymmetric hydrolysis
Cu-MOF	Microperoxidase-11	Bio-catalysis
CYCU-4, UiO-66	Trypsin	BSA digestion
NU-1003, PCN-128y	Anhydrolase	Detoxifying DFP and Soman
MIL-101-NH_2	Hemin	Bio-sensing
HKUST-1	Lipase	Esterification

nium/ruthenium NPs) denoted a better ablation of cancer [395]. Apart from ZIF-90 and ZIF-8 the delivery of MOF modulated CRISPR/Cas9 genome system, has a special impact towards the treatment of the diseases [396–398].

4.12. Imaging

This is the phenomenon associated with a prior diagnosis and observation of several ailments leading to impart on time precaution as well as treatment. Numerous imaging technologies like CT, MRI, PAI (Photoacoustic imaging), PET (positron emission tomography) and optical imaging associated with MOFs as the carrier for contrasting or imaging agents were being widely explored for several theranostics [398].

5. Challenges, solutions and future directions

Despite of the exceptional properties of MOFs towards disease theranostics, still they face several challenges in their applications. Very few clinical studies have been reported on their biological approaches, stability, degradability, half-life, blood circulation, and it should be more emphasized on their characteristics such as imaging/controlled release/sensing efficiency. The lack of systematic assessment for MOFs efficiency, limits their level of understanding for biological solicitations [399]. However, synthesizing MOFs derived monodisperse formulations with utmost stability remains a critical delinquent. A strict evaluation for surface modification is highly desirable for predicting a better stealth of the surface-engineered NPs [400]. More emphasis could be concerted towards a better biocompatibility, pharmacokinetics, bio distribution and toxicological (*in vivo*/*in vitro*) analysis of MOFs, from the preclinical and clinical perspectives [401]. The extensive research is needed for establishing a solid mechanism based performance of MOFs prior to its clinical enactment [399]. Hopefully, MOFs are going to be considered as the most promising elements in future nano biomedicine, and will pave maximum attention towards the advanced materials research on the field of nano-biotechnology [402].

Despite of a large number of prospective of the MOFs and MOF-modulated composites towards the biomedical field, specifically towards biomedicine (such as high atomic utilization, better specific surface area, PDA, PTA, regulating the release of antibacterial agents by modulating their morphology and size), their status is still in a preliminary stage of research, with ampoules of challenges and issues need to be rectified. MOFs developed from metal ions associated with organic ligands, are degradable up to certain extent. However, the impact of the developed by-products from their biotransformation is yet another mystery and till date has not been clarified properly [403]. Nevertheless, the researchers have studied the antibacterial activities of single-atom enzymes with multiple number of active sites after synthesizing them. Thus, the exploration of the antibacterial mechanisms targeted *via* altered active sites might be providing better futuristic aspects for enriching the knowledge of safety and effectiveness on numerous active sites of MOF [403]. The biosafety of such MOF based composites are another concern for successful allotment of these weapons in numerous biomedical and clinical approaches [404]. The mechanisms of NZs at multiple enzyme responses are to be explored along with the optimization of their specificity and selectivity [405–408].

6. Conclusions and perspectives

This review is highlighted with the applications of MOF-derived NZ as antibacterial, ROS scavenging, bio sensing, bio imaging, pollutant treatment and cancer therapy. NZ are advantageous with high stability, low-cost synthesis, better reusability, and having better performance under several critical conditions compared to their natural ancestors. Different aspects of MOF-modulated NZ mimicking responses (peroxidases, SOD, oxidases, hydrolases and catalases), along with solvothermal treatment, *in situ* growth, and

pyrolysis have been discussed. Several factors such as dimension, pore size, pH, temperature, constitution and modification of MOF-based NZ towards their catalytic activity were narrated. The review reported the diversified applications of MOF-based NZ in different biomedical and environmental control segments. They have been deployed as sensors for detection of several ions or biomolecules in different theranostic approaches. Being an emerging field, the MOF-based NZ tailored with several metal NPs and metal oxides are highly potential towards different catalytic responses. In contrast, MOF-based NZ are found to be functionally stable at extreme/diversified temperatures and pH conditions. MOFs based surface modification leads to develop a better adsorption and intrinsic catalytic efficacy in cascade of catalytic reactions. Till date, the synthetic strategy of MOF-modulated hetero atom-doped NZ (*i.e.*, single-atom/single-site NZ), is restricted with ZIF series (as starting material), but however, the discovery of some different strategies towards MOFs doping leads to control over the microstructure, distribution, and contents of the hetero atoms. Apart from the synchrotron radiation X-ray absorption spectroscopy (only providing information regarding the coordination numbers) several advanced characterization technologies (*in situ*) like femtosecond-laser spectroscopy as well as scanning tunneling microscopy (*in situ*) could be applied for spatial and temporal prediction of interactions processed between substrates and catalytic active sites. Moreover, the rational integration of DFT simulations could provide an in-depth indulgent of the mechanisms, thereby guiding the synthesis of super active NZ. Though NZ towards detection of biomolecules have been applied to a certain extent, but still to be explored in various domains like environmental protection (*e.g.*, elimination of pollutants and water treatments) and public health (*e.g.*, antiviral, anti-cancer and antibacterial therapy) with a desired skill. Lastly, in order to avail success in biological applications, the NZ need to be focused on achieving utmost biocompatibility prior to their preclinical/clinical translation as a replacement of natural enzymes for a global industrial exploration. For a successful practical approach, it is highly recommended to consider a rapid kinetic analysis, excellent selection criteria, better adsorption capacity, extraordinary rejuvenation and reusability, and production scale-up for environmental supremacy.

Declaration of competing interest

The authors declare that they have no known competing financial interests or personal relationships that could have appeared to influence the work reported in this paper.

References

[1] N. Stasyuk, O. Smutok, O. Demkiv, et al., Sensors 20 (2020) 1–42.
[2] A.M. Ashrafi, Z. Bytesnikova, J. Barek, L. Richtera, V. Adam, Biosen. Bioelectron. 192 (2021) 113494.
[3] N. Stasyuk, O. Smutok, O. Demkiv, et al., Sensors 20 (2020) 4509.
[4] X. Huang, S. Zhang, Y. Tang, et al., Coord. Chem. Rev. 449 (2021) 1–24.
[5] M. Liang, X. Yan, Acc. Chem. Res. 52 (2019) 2190–2200.
[6] H. Wei, E. Wang, Chem. Soc. Rev. 42 (2013) 6060–6093.
[7] S.S. Lucky, K.C. Soo, Y. Zhang, Chem. Rev. 115 (2015) 1990–2042.
[8] Y. Gao, Y. Zhou, R. Chandrawati, ACS. Appl. Nano Mater. 3 (2020) 1–21.
[9] M.H. Hassan, D. Andreescu, S. Andreescu, ACS. Appl. Nano Mater. 3 (2020) 3288–3294.
[10] N. Singh, G. Mugesh, Angew. Chem. Int. Ed. 58 (2019) 7797–7801.
[11] H. Sun, Y.A. Zhou, J. Ren, X. Qu, Angew. Chem. Int. Ed. 57 (2018) 9224–9237.
[12] L. Ma, M.i. Zhou, C. He, et al., Green Chem. 21 (2019) 4887–4918.
[13] Q. Tang, S. Cao, T. Ma, et al., Adv. Funct. Mater. 31 (2021) 1–29.
[14] H. Dong, Y. Fan, W. Zhang, N. Gu, Y. Zhang, Bioconjug. Chem. 30 (2019) 1273–1296.
[15] H. Wang, K. Wan, X. Shi, Adv. Mater. 31 (2019) 1–10.
[16] H.S. Wang, Coord. Chem. Rev. 349 (2017) 139–155.
[17] X. Tao, X. Wang, B. Liu, J. Liu, Biosens. Bioelectron. 168 (2020) 1–14.
[18] M. Yuan, X. Guo, N. Li, et al., Sens. Actuator B: Chem. 297 (2019) 126809.
[19] B. Xu, H. Wang, W. Wang, et al., Angew. Chem. Int. Ed. 58 (2019) 4911–4916.
[20] W. Song, B. Zhao, C.e. Wang, Y. Ozaki, X. Lu, J. Mater. Chem. B 7 (2019) 850–875.
[21] L. Hou, G. Jiang, Y. Sun, et al., Catalysts 9 (2019) 1–17.
[22] T. Wang, P. Su, F. Lin, Y. Yang, Y. Yang, Sens. Actuator B: Chem. 254 (2018) 329–336.
[23] H. Li, T. Wang, Y. Wang, et al., Indus. Eng. Chem. Res. 57 (2018) 2416–2425.
[24] S. Wu, D. Guo, X. Xu, J. Pan, X. Niu, Sens. Actuator B: Chem. 303 (2020) 1–8.
[25] Y. Xu, J. Xue, Q. Zhou, et al., Angew. Chem. Int. Ed. 59 (2020) 14498–14503.
[26] J. Liang, Z. Liang, R. Zou, Y. Zhao, Adv. Mater. 29 (2017) 1701139.
[27] C.L. Tan, L.Z. Zhao, P. Yu, Angew. Chem. Int. Ed. 56 (2017) 7842–7846.
[28] L. Zhao, W. Yuan, J. Li, et al., Adv. Funct. Mater. 28 (2018) 1806162.
[29] J. Wu, X. Wang, Q. Wang, Chem. Soc. Rev. 48 (2019) 1004–1076.
[30] Y. Huang, J. Ren, X. Qu, Chem. Rev. 119 (2019) 4357–4412.
[31] B. Yang, Y. Chen, J. Shi, Adv. Mater. 31 (2019) 1901778.
[32] D. Wang, D. Jana, Y. Zhao, Acc. Chem. Res. 53 (2020) 1389–1400.
[33] Y. Qiu, G. Tan, Y. Fang, New J. Chem. 45 (2021) 20987–21000.
[34] Y. Cui, B. Li, H. He, et al., Acc. Chem. Res. 49 (2016) 483–493.
[35] X. Gong, Y. Shu, Z. Jiang, et al., Angew. Chem. Int. Ed. 132 (2020) 5364–5369.
[36] J. Liu, J. Huang, L. Zhang, J. Lei, Chem. Soc. Rev. 50 (2021) 1188–1218.
[37] X. Li, S. Ding, X. Xiao, et al., J. Mater. Chem. A 5 (2017) 12774–12781.
[38] Z. Zhao, J. Ding, R. Zhu, H. Pang, J. Mater. Chem. A 7 (2019) 15519–15540.
[39] Y. Xu, S. Zheng, H. Tang, et al., Energy Storage Mater. 9 (2017) 11–30.
[40] X. Zhang, G. Li, D. Wu, Biosens. Bioelectron. 137 (2019) 178–198.
[41] M. Zhu, X. Wu, B. Niu, H. Guo, Y. Zhang, Appl. Organomet. Chem. 32 (2018) e4333.
[42] S. Abedi, A.A. Tehrani, A. Morsali, New. J. Chem. 39 (2015) 5108–5111.
[43] P. Tong, J. Liang, X. Jiang, J. Li, Crit. Rev. Anal. Chem. 50 (2020) 376–392.
[44] Y. Wang, J. Yan, N. Wen, Biomaterials 230 (2020) 119619.
[45] Y. Pan, S. Zhan, F. Xia, Anal. Biochem. 546 (2018) 5–9.
[46] T.T. Han, J. Yang, Y.Y. Liu, J.F. Ma, Microp. Mesopor. Mater. 228 (2016) 275–288.
[47] T.T. Han, H.L. Bai, Y.Y. Liu, J.F. Ma, J. Solid State Chem. 269 (2019) 588–593.
[48] P. Ling, J. Lei, H. Ju, Biosens. Bioelectron. 71 (2015) 373–379.
[49] J. Zhang, L. Sun, C. Chen, et al., Alloys Compd. 695 (2017) 520–525.
[50] H.J. Buser, D. Schwarzenbach, W. Petter, A.J.I.C. Ludi, Inorg. Chem. 16 (1977) 2704–2710.
[51] K. Hirai, K. Sumida, M. Meilikhov, J. Mater. Chem. C 2 (2014) 3336–3344.
[52] N. Yanai, K. Kitayama, Y. Hijikata, Nat. Mater. 10 (2011) 787–793.
[53] J.W. Ye, X.Y. Li, H.L. Zhou, J.P. Zhang, Sci. China Chem. 62 (2019) 341–346.
[54] J.H. Cavka, S. Jakobsen, U.J. Olsbye, Am. Chem. Soc. 130 (2008) 13850–13851.
[55] J.S. Seo, D. Whang, H. Lee, Nature 404 (2000) 982–986.
[56] O.V. Gutov, W. Bury, D.A. Gomez-Gualdron, Chem. Eur. J. 20 (2014) 12389–12393.
[57] S. Yang, J. Sun, A.J. Ramirez-Cuesta, Nat. Chem. 4 (2012) 887–894.
[58] R. Grunker, V. Bon, P. Muller, Chem. Commun. 50 (2014) 3450–3452.
[59] T. Ahnfeldt, N. Guillou, D. Gunzelmann, et al., Angew. Chem. Int. Ed. 48 (2009) 5163–5166.
[60] S.S.Y. Chui, S.M.F. Lo, J.P. Charmant, A.G. Orpen, I.D. Williams, Science 283 (1999) 1148–1150.
[61] S.S. Nadar, L. Vaidya, S. Maurya, V.K. Rathod, Coord. Chem. Rev. 396 (2019) 1–21.
[62] V.F. Yusuf, N.I. Malek, S.K. Kailasa, ACS Omega 7 (2022) 44507–44531.
[63] D. Jiang, D. Ni, Z.T. Rosenkrans, et al., Chem. Soc. Rev. 48 (2019) 3683–3704.
[64] Y. Hu, H. Cheng, X. Zhao, et al., ACS Nano 11 (2017) 5558–5566.
[65] X. Yang, J.K. Sun, M. Kitta, H. Pang, Q. Xu, Nat. Catal. 1 (2018) 214–220.
[66] K. Liang, C.J. Coghlan, S.G. Bell, C. Doonan, P. Falcaro, Chem. Commun. 52 (2016) 473–476.
[67] D. Feng, T.F. Liu, J. Su, et al., Nat. Commun. 6 (2015) 1–8.
[68] L. Jiao, G. Wan, R. Zhang, H. Zhou, S.H. Yu, Angew. Chem. Int. Ed. 57 (2018) 8525–8529.
[69] L. Wang, S. Li, X. Zhang, Y. Huang, Talanta 216 (2020) 121009.
[70] X. Zhao, P. Pachfule, S. Li, J.R.J. Simke, J. Schmidt, Angew. Chem. Int. Ed. 57 (2018) 8921–8926.
[71] X.F. Lu, L. Yu, X.W. Lou, Sci. Adv. 5 (2019) 1–10.
[72] S. Dang, Q.L. Zhu, Q. Xu, Nat. Rev. Mater. 3 (2018) 17075.
[73] W. Gong, Y. Lin, C. Chen, et al., Adv. Mater. 31 (2019) 1808341.
[74] X. Niu, Q. Shi, W. Zhu, et al., Biosens. Bioelectron. 142 (2019) 111495.
[75] S. Singh, Front. Chem. 7 (2019) 1–10.
[76] L. Gao, K.M. Giglio, J.L. Nelson, H. Sondermann, A.J. Travis, Nanoscale 6 (2014) 2588–2593.
[77] L. Su, Y. Xiong, H. Yang, P. Zhang, F. Ye, J. Mater. Chem. B 4 (2016) 128–134.
[78] Y. Xu, B. Li, S. Zheng, et al., J. Mater. Chem. A 6 (2018) 22070–22076.
[79] Q. Li, Z. Shao, T. Han, M. Zheng, H. Pang, Chem. Eng. 7 (2019) 8986–8992.
[80] W. Zhou, H. Li, B. Xia, Nano Res. 11 (2018) 5761–5768.
[81] L. Han, H. Zhang, D. Chen, F. Li, Adv. Funct. Mater. 28 (2018) 1800018.
[82] M. Li, J. Chen, W. Wu, Y. Fang, S. Dong, J. Am. Chem. Soc. 142 (2020) 15569–15574.
[83] Q. Chen, X. Zhang, S. Li, J. Tan, C. Xu, Chem. Eng. J. 395 (2020) 125130.
[84] Y. Liu, X. Wang, H. Wei, Analyst 145 (2020) 4388–4397.
[85] F. Cao, Y. Zhang, Y. Sun, Chem. Mater. 30 (2018) 7831–7839.
[86] X. Pan, L. Bai, H. Wang, Adv. Mater. 30 (2018) 1800180.
[87] J. Li, T. Li, D. Gorin, et al., Colloids Surf. A: Physicochem. Eng. Asp. 601 (2020) 124990.
[88] M. Zhang, F. Wu, W. Wang, et al., Chem. Mater. 31 (2019) 1847–1859.
[89] D.W. Zheng, Q.i. Lei, J.Y. Zhu, et al., Nano Lett. 17 (2017) 284–291.
[90] D. Wang, Y. Zhao, Chem 7 (2021) 2635–2671.
[91] K. Ye, L. Wang, H. Song, X. Li, X. Niu, J. Mater. Chem B 7 (2019) 4794–4800.
[92] S. Shams, W. Ahmad, A.H. Memon, et al., RSC Adv. 9 (2019) 40845–40854.

[93] M. Comotti, C. DellaPina, R. Matarrese, M. Rossi, Angew. Chem. Int. Ed. 43 (2004) 5812–5815.
[94] L. He, Q. Ni, J. Mu, J. Am. Chem. Soc. 142 (2020) 6822–6832.
[95] J. Wu, Z. Wang, X. Jin, et al., Adv. Mater. 33 (2021) 2005024.
[96] X. Xiao, G. Zhang, Y. Xu, et al., J. Mater. Chem. A 7 (2019) 17266–17271.
[97] Y. Ding, H. Xu, C. Xu, Adv. Sci. 7 (2020) 2001060.
[98] H. Chen, T. Yang, F. Liu, W. Li, Sens. Actuator B: Chem. 286 (2019) 401–407.
[99] Y. Wang, Y. Wang, L.I. Zhang, C.S. Liu, H. Pang, Inorg. Chem. Front. 6 (2019) 2514–2520.
[100] S. Li, L. Wang, X. Zhang, H. Chai, Y. Huang, Sens. Actuator B: Chem. 264 (2018) 312–319.
[101] Q. Chen, S. Li, Y. Liu, Sens. Actuator B: Chem. 305 (2020) 127511.
[102] S. Li, Y. Hou, Q. Chen, et al., ACS Appl. Mater. Interfaces 12 (2020) 2581–2590.
[103] P. Li, Q. Chen, T.C. Wang, et al., Chem 4 (2018) 1022–1034.
[104] Z. Zhao, Y. Huang, W. Liu, F. Ye, S. Zhao, ACS Sustain. Chem. Eng. 8 (2020) 4481–4488.
[105] W. Xu, L. Jiao, H. Yan, ACS. Appl. Mater. Interfaces 11 (2019) 22096–22101.
[106] X. Zhong, H. Xia, W. Huang, Z. Li, Y. Jiang, Chem. Eng. J. 381 (2020) 122758.
[107] I. Nath, J. Chakraborty, F. Verpoort, Chem. Soc. Rev. 45 (2016) 4127–4170.
[108] M. Li, H. Zhang, Y. Hou, et al., Nanoscale. Horiz. 5 (2020) 202–217.
[109] C. Zhao, Z. Jiang, R. Mu, Y. Li, Talanta 159 (2016) 365–370.
[110] H. Ranji-Burachaloo, F. Karimi, K. Xie, et al., ACS Appl. Mater. Interfaces 9 (2017) 33599–33608.
[111] H. Cheng, Y. Liu, Y. Hu, et al., Anal. Chem. 89 (2017) 11552–11559.
[112] H. Jin, D. Ye, L. Shen, et al., Analytic. Chem. 94 (2022) 1499–1509.
[113] C. Fu, H. Zhou, L. Tan, ACS. Nano 12 (2018) 2201–2210.
[114] T. Zhang, Y. Xing, Y.U. Song, Anal. Chem. 91 (2019) 10589–10595.
[115] Z.W. Jiang, F.Q. Dai, C.Z. Huang, Y.F. Li, RSC Adv. 6 (2016) 86443–86446.
[116] J. He, Y. Zhang, X. Zhang, Y. Huang, Sci. Rep. 8 (2018) 1–8.
[117] F.F. Chen, Y.J. Zhu, Z.C. Xiong, T.W. Sun, Chem. Eur. J. 23 (2017) 3328–3337.
[118] M.A. Komkova, E.E. Karyakina, A.A. Karyakin, J. Am. Chem. Soc. 140 (2018) 11302–11307.
[119] F. Cui, Q. Deng, L. Sun, RSC Adv. 5 (2015) 98215–98221.
[120] F.K. Shieh, S.C. Wang, C. Yen, J. Am. Chem. Soc. 137 (2015) 4276–4279.
[121] X. Lian, Y. Fang, E. Joseph, Chem. Soc. Rev. 46 (2017) 3386–3401.
[122] Z. He, X. Huang, C. Wang, Angew. Chem. Int. Ed. 58 (2019) 8752–8756.
[123] J. Liu, Q. Chen, W. Zhu, Adv. Funct. Mater. 27 (2017) 1605926.
[124] D. Wang, H. Wu, W. Lim, Adv. Mater. 31 (2019) 1901893.
[125] J. Liu, T. Liu, P. Du, L. Zhang, J. Lei, Angew. Chem. Int. Ed. 58 (2019) 7808–7812.
[126] S. Cao, K. Zhang, B. Hanna, E. Al-Sayed, Chin. Chem. Lett. 33 (2022) 1757–1762.
[127] Y. Yang, D. Zhu, Y. Liu, Nanoscale 12 (2020) 13548–13557.
[128] G.A. Keller, T.G. Warner, K.S. Steimer, R.A. Hallewell, Proc. Natl. Acad. Sci. U. S. A. 88 (1991) 7381–7385.
[129] L. Zhang, Y. Zhang, Z. Wang, Mater. Horiz. 6 (2019) 1682–1687.
[130] W. Zhang, S. Hu, J.J. Yin, et al., J. Am. Chem. Soc. 138 (2016) 5860–5865.
[131] S.L. Cao, D.M. Yue, X.H. Li, ACS Sustain. Chem. Eng. 4 (2016) 3586–3595.
[132] K.P. Bhabak, G. Mugesh, Acc. Chem. Res. 43 (2010) 1408–1419.
[133] N. Singh, M.A. Savanur, S. Srivastava, P. D'Silva, G. Mugesh, Angew. Chem. Int. Ed. 56 (2017) 14267–14271.
[134] J. Wu, Y. Yu, Y. Cheng, et al., Angew .Chem. Int. Ed. 60 (2021) 1227–1234.
[135] Z. Zhao, T. Lin, W. Liu, et al., Spectrochim. Acta A 219 (2019) 240–247.
[136] Y. Huang, M. Zhao, S. Han, Adv. Mater. 29 (2017) 1700102.
[137] H. Yang, R. Yang, P. Zhang, Microchim. Acta 184 (2017) 4629–4635.
[138] L. Luo, L. Huang, X. Liu, et al., Inorg. Chem. 58 (2019) 11382–11388.
[139] B. Liu, H. Shioyama, T. Akita, Q.J. Xu, Am. Chem. Soc. 130 (2008) 5390–5391.
[140] L. Zhang, Z.J. Xia, Phys. Chem. C 115 (2011) 11170–11176.
[141] M. Bilal, N. Khaliq, M. Ashraf, et al., Colloid Surf. B. Biointerface 221 (2023) 112950.
[142] K. Fan, J. Xi, L. Fan, et al., Nat. Commun. 9 (2018) 1440.
[143] R. Fasan, ACS Catal. 2 (2012) 647–666.
[144] S. Liu, Z. Li, C. Wang, Nat. Commun. 11 (2020) 938.
[145] P. Jiang, S. Chen, C. Wang, Mater. Today Sustain. 9 (2020) 100039.
[146] C. Wang, D. Wang, S. Liu, J. Catal. 389 (2020) 150.
[147] M. Chan, B.G. Chen, W.T. Huang, et al., Mater. Today Adv. 17 (2023) 100342.
[148] W. Ma, J. Mao, X. Yang, Chem. Commun. 55 (2019) 159–162.
[149] M. Huo, L. Wang, Y. Wang, ACS Nano 13 (2019) 2643–2653.
[150] L. Gao, J. Zhuang, L. Nie, Nat. Nanotechnol. 2 (2007) 577–583.
[151] F. Natalio, R. Andre, A.F. Hartog, Nat. Nanotechnol. 7 (2012) 530–535.
[152] N. Singh, M.A. Savanur, S. Srivastava, Angew. Chem. Int. Ed. 56 (2017) 14267–14271.
[153] S. Wang, Y. Jin, W. Ai, Nano Res. (2023) 1–10.
[154] H. Chen, X. Zeng, H.P. Tham, et al., Angew. Chem. Int. Ed. 58 (2019) 7641–7646.
[155] G. Yang, S.Z.F. Phua, W.Q. Lim, et al., Adv. Mater. 31 (2019) 1901513.
[156] S.Z.F. Phua, C. Xue, W.Q. Lim, et al., Chem. Mater. 31 (2019) 3349–3358.
[157] H.P. Tham, K. Xu, W.Q. Lim, et al., ACS Nano 12 (2018) 11936–11948.
[158] S. Dang, Q. Zhu, Q. Xu, Nat. Rev. Mater. 3 (2018) 17075.
[159] A.J. Amali, H. Hoshino, C. Wu, et al., Chem. Eur. J. 20 (2014) 8279–8282.
[160] X. Deng, R. Zhao, Q. Song, et al., Drug. Deliv. 29 (2022) 3142–3154.
[161] S. Yu, K. Xu, Z. Wang, Z. Zhang, Z. Zhang, Front. Bioengin. Biotechnol. 10 (2023) 1–14.
[162] K. Zhang, L. Lu, Z. Liu, et al., Colloid. Surf. A: Physicochem. Eng. Asp. 650 (2022) 129662.
[163] M. Huo, L. Wang, Y. Wang, et al., Adv. Mater. 32 (2020) e2003563.
[164] M. Huo, L. Wang, Y. Chen, et al., Nat. Commun. 8 (2017) 357.
[165] W. Zhou, J. Gao, H. Zhao, et al., Environ. Technol. 38 (2017) 1887–1896.
[166] A.L. Pham, F.M. Doyle, D.L. Sedlak, Water. Res. 46 (2012) 6454–6462.
[167] S. Fu, S. Wang, X. Zhang, Colloid Surf. B 154 (2017) 239–245.
[168] B. Wang, J.J. Yin, X. Zhou, et al., J. Phys. Chem. C 117 (2012) 383–392.
[169] Z. Chen, J. Yin, Y. Zhou, et al., ACS Nano 6 (2012) 4001–4012.
[170] S. Zhao, H. Duan, Y. Yang, et al., Nano Lett. 19 (2019) 8887–8895.
[171] Y. Chen, T. Chen, X. Wu, et al., Small 15 (2019) e1903153.
[172] D. Ni, D. Jiang, C. Kutyref, et al., Nat. Commun. 18 (2018) 5421.
[173] S. Li, D. Jiang, E.B. Ehlerding, et al., ACS Nano 13 (2019) 13382–13389.
[174] Y. Zhang, D. Li, J. Tan, et al., Small 17 (2021) e2005739.
[175] C. Ren, D. Li, Q. Zhou, et al., Biomaterials 232 (2020) 119752.
[176] Q. Han, X. Wang, X. Liu, et al., J. Colloid Interf. Sci. 539 (2019) 575–584.
[177] X. Hu, F. Li, F. Xia, et al., J. Am. Chem. Soc. 142 (2019) 1636–1644.
[178] L. Feng, Z. Dong, C. Liang, et al., Biomaterials 181 (2018) 81–91.
[179] W. Zhen, Y. Liu, L. Lin, et al., Angew. Chem. Int. Ed. 57 (2018) 10309–103013.
[180] P. Xu, X. Wang, T. Li, et al., Nanoscale 12 (2020) 4051–4060.
[181] H. Su, D.D. Liu, M. Zhao, et al., ACS Appl. Mater. Interfaces 7 (2015) 8233–8242.
[182] D.Y. Zhang, M.R. Younis, H. Liu, et al., Biomaterials 271 (2021) 120706.
[183] X. Ren, D. Chen, T. Wang, et al., J. Nanobiotechnol. 20 (2022) 92.
[184] G. Merga, N. Saucedo, L.C. Cass, et al., J. Phys. Chem. C 114 (2010) 14811–14818.
[185] S. Wang, W. Chen, A.L. Liu, et al., Chem. Phys. Chem. 13 (2012) 1199–1204.
[186] Y. Lin, Z. Li, Z. Chen, J. Ren, X. Qu, Biomaterials 34 (2013) 2600–2610.
[187] R.V. Jagadeesh, K. Murugesan, A.S. Alshammari, Science 358 (2017) 326–332.
[188] S. Li, L. Wang, X. Zhang, et al., Sens. Actuator B 264 (2018) 312–319.
[189] Y. Song, D. Cho, S. Venkateswarlu, M. Yoon, RSC Adv. 7 (2017) 10592–10600.
[190] O. Karagiaridi, W. Bury, J.E. Mondloch, J.T. Hupp, O.K. Farha, Angew. Chem. Int. Ed. 53 (2014) 4530–4540.
[191] M.J. Katz, S.Y. Moon, J.E. Mondloch, Chem. Sci. 6 (2015) 2286–2291.
[192] O. Karagiaridi, J. Lalonde, Am. Chem. Soc. 134 (2012) 18790–18796.
[193] Y. Sang, L. Cao, J. Am. Chem. Soc. 142 (2020) 5177–5183.
[194] K. Wang, D. Feng, T. Liu, Am. Chem. Soc. 136 (2014) 13983–13986.
[195] J.D. Evans, C.J. Sumby, C.J. Doonan, et al., Chem. Soc. Rev. 43 (2014) 5933–5951.
[196] W.H. Chen, M. Vazquez-Gonzalez, A. Kozell, A. Cecconello, I. Willner, Small 14 (2018) 1703149.
[197] A.H. Valekar, B.S. Batule, M.I. Kim, et al., Biosens. Bioelectron. 100 (2018) 161–168.
[198] L. He, Y. Li, Q. Wu, et al., ACS Appl. Mater. Interfaces 11 (2019) 29158–29166.
[199] D. Yang, H. Yu, T. He, et al., Nat. Commun. 10 (2019) 3844.
[200] D. Wang, H. Wu, S.Z.F. Phua, et al., Nat. Commun. 11 (2020) 357.
[201] Z. Zhao, J. Pang, W. Liu, et al., Microchim. Acta 186 (2019) 295.
[202] Q. Wang, X. Zhang, L. Huang, Angew. Chem. Int. Ed. 56 (2017) 16082–16085.
[203] X.Q. Tang, Y.D. Zhang, Z.W. Jiang, Talanta 179 (2018) 43–50.
[204] Q. Zhang, F. Zhang, L. Yu, et al., Microchim. Acta 187 (2020) 1–8.
[205] J. Zhang, J. Liu, Luminescence 35 (2020) 1185–1194.
[206] T. Lin, Y. Qin, Y. Huang, et al., Chem. Commun. 54 (2018) 1762–1765.
[207] M. Pamei, A.G. Achumi, R. Kahmei, et al., Microporous Mesoporous Mater. 340 (2022) 112031.
[208] A. Badoei-dalfard, N. Sohrabi, Z. Karami, G. Sargazi, Biosens. Bioelectron. 141 (2019) 111420.
[209] J. Wang, Y. Hu, Q. Zhou, et al., ACS Appl. Mater. Interfaces 11 (2019) 44466–44473.
[210] L. Liang, Y. Huang, W. Liu, W. Zuo, F. Ye, Front. Chem. 8 (2020) 1–9.
[211] J.W. Zhang, H.T. Zhang, Z.Y. Du, et al., Chem. Commun. 50 (2014) 1092–1094.
[212] H. Tan, Q. Li, Z. Zhou, Anal. Chim. Acta 856 (2015) 90–95.
[213] Y. Zhang, J. Song, W. Shao, J. Microporous Mesoporous Mater. 310 (2021) 110642.
[214] H.J. Cheon, Q.H. Nguyen, M.I. Kim, Nanomaterials 11 (2021) 1207.
[215] J. Guo, S. Wu, Y. Wang, M. Zhao, Sens. Actuator. B: Chem. 312 (2020) 128021.
[216] J. Hassanzadeh, A. Khataee, H. Eskandari, Sens. Actuator. B: Chem. 259 (2018) 402–410.
[217] S. Wang, W. Deng, L. Yang, et al., ACS Appl. Mater. Interfaces 9 (2017) 24440–24445.
[218] N. Cheng, C. Zhu, Y. Wang, et al., J. Anal. Testing 3 (2019) 99–106.
[219] H. Li, H. Liu, J. Zhang, et al., ACS Appl. Mater. Interfaces 9 (2017) 40716–40725.
[220] C. Wang, G. Tang, H. Tan, Microchim. Acta 185 (2018) 1–8.
[221] C. Li, J. Hai, L. Fan, et al., Sens. Actuator. B: Chem. 284 (2019) 213–219.
[222] Q. Liu, A. Zhang, R. Wang, et al., Nano-Micro Lett. 13 (2021) 1–53.
[223] L. Wang, Z. Hu, S. Wu, et al., Anal. Chim. Acta 1121 (2020) 26–34.
[224] X. Ruan, D. Liu, X. Niu, et al., Anal. Chem. 91 (2019) 13847–13854.
[225] Y. Wang, Y. Zhu, A. Binyam, et al., Biosens. Bioelectron. 86 (2016) 432–438.
[226] S. Li, X. Hu, Q. Chen, et al., Biosens. Bioelectron. 137 (2019) 133–139.
[227] X. Wang, X. Jiang, H. Wei, J. Mater. Chem. B 8 (2020) 6905–6911.
[228] C. Wang, J. Gao, Y. Cao, H. Tan, Anal. Chim. Acta 1004 (2018) 74–81.
[229] C. Song, W. Ding, H. Liu, et al., New J. Chem. 43 (2019) 12776–12784.
[230] X. Li, X. Li, D. Li, et al., Biosens. Bioelectron. 168 (2020) 112554.
[231] D. Sun, Z. Luo, J. Lu, et al., Biosens. Bioelectron. 134 (2019) 49–56.
[232] P. Ling, C. Qian, J. Yu, F. Gao, Biosens. Bioelectron. 149 (2020) 111838.
[233] S.R. Hormozi Jangi, M. Akhond, Microchem. J. 158 (2020) 105328.
[234] Y. Wu, Y. Ma, G. Xu, et al., Sens. Actuator B: Chem. 249 (2017) 195–202.
[235] T.K. Pal, Mater. Chem. Front. 7 (2023) 405–441.
[236] H. Tan, C. Ma, L. Gao, et al., Chem. Eur. J. 20 (2014) 16377–16383.

[237] L. Hou, Y. Qin, T. Lin, et al., Sens. Actuator B: Chem. 321 (2020) 128547.
[238] T. Wen, G. Quan, B. Niu, et al., Small 17 (2021) 2005064.
[239] L. Ma, F. Jiang, X. Fan, et al., Adv. Mater. 32 (2020) 2003065.
[240] D.Q. Chen, D.Z. Yang, C.A. Dougherty, et al., ACS Nano 11 (2017) 4315–4327.
[241] M. Cai, G. Chen, L. Qin, et al., Pharmaceutics 12 (2020) 232.
[242] R. Masoudifar, N. Pouyanfar, D. Liu, et al., Appl. Mat. Today 29 (2022) 101646.
[243] B. Maranescu, A. Visa, Int. J. Mol. Sci. 18 (2022) 4458.
[244] J. Park, Q. Jiang, D.W. Feng, L.Q. Mao, H.C. Zhou, J. Am. Chem. Soc. 138 (2016) 3518–3525.
[245] D. Duan, H. Liu, M. Xu, ACS Appl. Mater. Interfaces 10 (2018) 42165–42174.
[246] Y.A. Li, X.D. Zhao, H.P. Yin, et al., Chem. Commun. 52 (2016) 14113–14116.
[247] M.F. Attia, J. Pharm. Pharmacol. 71 (2019) 1185–1198.
[248] F.S. Anarjan, Nano. Struct. Nano Objects 19 (2019) 100370.
[249] M.J. Akhtar, Clin. Chim. Acta 436 (2014) 78–92.
[250] J. Yoo, Cancers (Basel) 11 (2019) 640.
[251] C. Fang, Z. Deng, G. Cao, et al., Adv. Funct. Mater. 30 (2020) 1910085.
[252] Z. Tian, K. Yang, T. Yao, et al., Small 15 (2019) 1903746.
[253] J. Li, K. Yi, Y. Lei, et al., Chem. Commun. 56 (2020) 6285–6288.
[254] H.B. Ji, C.R. Kim, C.H. Min, et al., Bioengin. Transl. Med. 8 (2023) e10477.
[255] C. Zhang, L. Zhang, W. Wu, Adv. Mater. 31 (2019) 1901179.
[256] K. Mahmoudi, K.L. Garvey, A. Bouras, J. Neurooncol. 141 (2019) 595–607.
[257] S. Ayan, G. Gunaydin, N. Yesilgul-Mehmetcik, Chem. Commun. 56 (2020) 14793–14796.
[258] S. Kwiatkowski, B. Knap, D. Przystupski, et al., Biomed. Pharmacother. 106 (2018) 1098–1107.
[259] E.Ö. Gündüz, M.E. Gedik, G. Günaydın, E. Okutan, Chem. Med. Chem. 17 (2022) e202100693.
[260] P. Sarbadhikary, B.P. George, H. Abrahamse, Theranostics 11 (2021) 9054–9088.
[261] C. Lennicke, H.M. Cochemé, Mol. Cells 81 (2021) 3691–3707.
[262] E. Piskounova, M. Agathocleous, M.M. Murphy, et al., Nature 527 (2015) 186–191.
[263] C. Prinz, E. Vasyutina, G. Lohmann, et al., Mol. Cancer 14 (2015) 114.
[264] G. Plotino, N.M. Grande, M. Mercade, Int. Endod. J. 52 (2019) 760–774.
[265] C. Donohoe, M.O. Senge, L.G. Arnaut, L.C. Gomes-Da-Silva, Biochim. Biophys. Acta Rev. Cancer 1872 (2019) 188308.
[266] X. Zhang, F. Peng, D. Wang, J. Function. Biomat. 13 (2022) 215.
[267] A. Sahu, I. Kwon, G. Tae, Biomaterials 228 (2020) 119578.
[268] Y. Zhang, F. Wang, C. Liu, et al., ACS Nano 12 (2018) 651–661.
[269] J.Y. Zeng, M.Z. Zou, M. Zhang, et al., ACS Nano 12 (2018) 4630–4640.
[270] G. Lan, K. Ni, S.S. Veroneau, J. Am. Chem. Soc. 141 (2019) 4204–4208.
[271] D. Wang, H. Wu, S.Z.F. Phua, et al., Nat. Commun. 11 (2020) 1–13.
[272] K. Zhang, X. Meng, Y. Cao, et al., Adv. Funct. Mater. 28 (2018) 1–10.
[273] X. Liu, Y. Pan, J. Yang, et al., Nano Res. 13 (2020) 653–660.
[274] Q. You, K. Zhang, J. Liu, Adv. Sci. 7 (2020) 1903341.
[275] H. Cheng, J.Y. Zhu, S.Y. Li, et al., Adv. Funct. Mater. 26 (2016) 7847–7860.
[276] W. Zhang, J. Lu, X. Gao, Angew. Chem. Int. Ed. 57 (2018) 4891–4896.
[277] S. Yin, G. Song, Y. Yang, et al., Adv. Funct. Mater. 29 (2019) 1901417.
[278] H. Min, J. Wang, Y. Qi, et al., Adv. Mater. 31 (2019) 1808200.
[279] S. Wang, L. Shang, L. Li, et al., Adv. Mater. 28 (2016) 8379–8387.
[280] J. Beik, Z. Abed, F.S. Ghoreishi, et al., J. Control. Rel. 235 (2016) 205–221.
[281] R. Bardhan, S. Lal, A. Joshi, N.J. Halas, Acc. Chem. Res. 44 (2011) 936–946.
[282] T. Zhao, S. Qin, L. Peng, et al., Carbohydr. Polym. 214 (2019) 221–233.
[283] W. Sheng, S. He, W.J. Seare, A. Almutairi, J. Biomed. Opt. 22 (2017) 80901.
[284] A.M. Alkilany, L.B. Thompson, S.P. Boulos, et al., Adv. Drug. Deliv. Rev. 64 (2012) 190–199.
[285] J. Li, X. Yu, Y. Jiang, et al., Adv. Mater. 33 (2021) e2003458.
[286] S. Kunjachan, A. Detappe, R. Kumar, et al., Nano Lett. 15 (2015) 7488–7496.
[287] H.K. Angell, D. Bruni, J.C. Barrett, et al., Clin. Cancer Res. 26 (2020) 332–339.
[288] D. Xu, J. Liu, Y. Wang, et al., ACS Biomater. Sci. Eng. 6 (2020) 4940–4948.
[289] C. Kong, X. Chen, Int. J. Nanomed. 17 (2022) 6427–6446.
[290] B.C. Wilson, R.A. Weersink, Photochem. Photobiol. 96 (2020) 219–231.
[291] C. Liu, L. Luo, L. Zeng, et al., Small 14 (2018) 1801851.
[292] X. Zeng, S. Yan, P. Chen, et al., Nano Res. 13 (2020) 1527–1535.
[293] Y. Zhao, C. Shi, J. Cao, Drug Deliv. 28 (2021) 2085–2099.
[294] S. Chen, Y. Yin, J. Appl. Mech. 81 (2014) 121002–121014.
[295] M. Elsabahy, G.S. Heo, S.M. Lim, G. Sun, K.L. Wooley, Chem. Rev. 115 (2015) 10967–11011.
[296] Y. Li, J. Jin, D. Wang, et al., Nano Res. 11 (2018) 3294–3305.
[297] Y. Liu, Z. Tang, Chem. Eur. J. 18 (2012) 1030–1037.
[298] C.Y. Sun, C. Qin, X.L. Wang, Dalton Trans. 41 (2012) 6906–6909.
[299] C. Koschnick, R. Stäglich, T. Scholz, et al., Nat. Commun. 12 (2021) 3099–3109.
[300] D. Chen, D. Yang, C.A. Dougherty, et al., ACS Nano 11 (2017) 4315–4327.
[301] M. Liu, G. Zeng, K. Wang, et al., Nanoscale 8 (2016) 16819–16840.
[302] J. Liu, Y. Yang, W. Zhu, et al., Biomaterials 97 (2016) 1–9.
[303] Y. Liu, K. Ai, L. Lu, Chem. Rev. 114 (2014) 5057–5115.
[304] J.A. Ibacache, J.A. Valderrama, V.J. Arancibia, Chil. Chem. Soc. 61 (2016) 3191–3194.
[305] K. Yang, L. Hu, X. Ma, Adv. Mater. 24 (2012) 1868–1872.
[306] Y.A. Cheon, J.H. Bae, B.G. Chung, Langmuir 32 (2016) 2731–2736.
[307] S. Lee, Y. Cho, H.K. Song, et al., Angew. Chem. Int. Ed. 124 (2012) 8878–8882.
[308] P. Ercius, O. Alaidi, M.J. Rames, G. Ren, J. Matthew, Adv. Mater. 27 (2015) 5638–5663.
[309] S. Li, L. Zhang, X. Liang, et al., Chem. Eng. J. 378 (2019) 122175–122181.
[310] S.K. Lee, Y. Zu, A. Herrmann, et al., J. Am. Chem. Soc. 121 (1999) 3513–3520.
[311] Y. Che, A. Datar, X. Yang, et al., J. Am. Chem. Soc. 129 (2007) 6354–6355.
[312] Y. Kai, H. Xu, C. Liang, et al., Adv. Mater. 24 (2012) 5586–5592.
[313] I. Ghosh, T. Ghosh, J.I. Bardagi, Science 346 (2014) 725–728.
[314] J. Park, D. Yuan, K.T. Pham, J. Am. Chem. Soc. 134 (2012) 99–102.
[315] L.L. Tan, H. Li, Y. Tao, Adv. Mater. 26 (2014) 7027–7031.
[316] X. Meng, B. Gui, D. Yuan, et al., Sci. Adv. 2 (2016) e1600480–e1600486.
[317] Y. Liu, J.F. Eubank, A.J. Cairns, et al., Angew. Chem. Int. Ed. 46 (2006) 3278–3283.
[318] A.J. Cairns, J. Eckert, L. Wojtas, et al., Chem. Mater. 28 (2016) 7353–7361.
[319] B. Seoane, S. Castellanos, A. Dikhtiarenko, Coord. Chem. Rev. 307 (2016) 147–187.
[320] C. Xuechao, D. Xiaoran, Chem. Eng. J. 358 (2019) 369–378.
[321] Z. Qin, D. Li, Y. Ou, et al., Crystal 13 (2023) 1–9.
[322] J. Feng, Z. Xu, P. Dong, et al., J. Mater. Chem. B 7 (2019) 994–1004.
[323] X. Yin, F. Ai, L. Han, Front. Chem. 10 (2022) 841316.
[324] L. Zhang, Z. Wang, Y. Zhang, et al., ACS Nano 12 (2018) 10201–10211.
[325] S.Y. Li, H. Cheng, B.R. Xie, et al., ACS Nano 11 (2017) 7006–7018.
[326] C. Liu, J. Xing, O.U. Akakuru, et al., Nano Lett. 19 (2019) 5674–5682.
[327] L. Dai, M. Yao, Z. Fu, Nat. Commun. 13 (2022) 2688.
[328] M. Wen, J. Ouyang, C. Wei, Angew. Chem. Int. Ed. 58 (2019) 17425–17432.
[329] Q. Chen, M. Chen, Z. Liu, et al., Chem. Soc. Rev. 48 (2019) 5506–5526.
[330] G. Lan, K. Ni, Z. Xu, et al., J. Am. Chem. Soc. 140 (2018) 5670–5673.
[331] K. Ni, G. Lan, C. Chan, et al., Nat. Commun. 9 (2018) 1–12.
[332] K. Ni, T. Aung, S. Li, et al., Chem 5 (2019) 1892–1913.
[333] X. Ma, X. Ren, X. Guo, et al., Biomaterials 214 (2019) 119223.
[334] Z. Deng, C. Fang, X. Ma, et al., ACS Appl. Mater. Interfaces 12 (2020) 20321–20330.
[335] L. Wang, C. Hou, H. Yu, et al., Chem. Electron. Chem. 7 (2020) 4446–4452.
[336] X. Chang, X. Li, X. Qiao, et al., Sens. Actuator. B: Chem. 304 (2020) 127430.
[337] X.F. Wang, W. Ma, F. Jiang, Chem. Eng. J. 338 (2018) 504–512.
[338] E.X. Chen, H. Yang, J. Zhang, Inorg. Chem. 53 (2014) 5411–5413.
[339] M. Gutiérrez, A.F. Möslein, J.C. Tan, ACS Appl. Mater. Interfaces 13 (2021) 7801–7811.
[340] L. Zhang, N. Wang, P. Cao, Microchem. J. 159 (2020) 105343.
[341] X. Wei, J. Guo, H. Lian, Sens. Actuator. B: Chem. 329 (2020) 129205.
[342] Y. Chen, P. Li, J.A. Modica, J. Am. Chem. Soc. 140 (2018) 5678–5681.
[343] Y. Zhou, L. Liu, Y. Cao, et al., ACS Appl. Mater. Interfaces 12 (2020) 22581–22592.
[344] C. Zhang, S. Hong, M.D. Liu, et al., J. Control. Rel. 320 (2020) 159–167.
[345] J. Xiao, S. Chen, J. Yi, et al., Adv. Funct. Mater. 27 (2017) 1604872.
[346] J. Xiao, Y. Zhu, S. Huddleston, et al., ACS Nano 12 (2018) 1023–1032.
[347] P. Zhang, Y. Li, Y. Tang, et al., ACS. Appl. Mater. Interfaces 12 (2020) 18319–18331.
[348] J. Li, F. Lv, J. Li, et al., Nano Res. 13 (2020) 2268–2279.
[349] S. Cai, W. Zhang, R. Yang, Nano Res. 15 (2023) 1–21.
[350] A.A. Farooqui, Neurochemical aspects of neurological disorders, Trace Amines and Neurological Disorders: Potential Mechanisms and Risk Factors, Elsevier Inc., Amsterdam, 2016, pp. 237–256.
[351] H.L. Chen, R.T. Li, K.Y. Wu, et al., Talanta 201 (2020) 120596.
[352] J. Zhu, Y. Tang, Y. Yang, et al., Microporous Mesoporous Mater. 288 (2019) 109610.
[353] D. Brambilla, B.L. Droumaguet, J. Nicolas, Nanomed. Nanotechnol. Biol. Med. 7 (2011) 521–540.
[354] Z. Liao, J. Zhang, E. Yu, Y. Cui, Polyhedron 151 (2018) 554–567.
[355] J. Zhao, F. Yin, L. Ji, et al., ACS Appl. Mater. Interfaces 12 (2020) 44447–44458.
[356] J. Wang, Y. Fan, Y. Tan, et al., ACS Appl. Mater. Interfaces 10 (2018) 36615–36621.
[357] A.E. Eldeeb, S. Salah, M.J. Ghorab, Drug. Deliv. Sci. Technol. 52 (2019) 236–247.
[358] J. He, C. Li, J. Ye, Y. Qiao, L. Gu, Biomed. Sign. Process. Cont. 67 (2021) 102491.
[359] W. Wang, A. Ge, H. Zhu, P. Yang, Inorg. Chim. Acta 506 (2020) 119526.
[360] X. Zhang, L. Fang, K. Jiang, et al., Biosens. Bioelectron. 130 (2019) 65–72.
[361] Z. Zhu, V. Natarajan, W.N.J. Wang, Solid. Stat. Chem. 288 (2020) 121434.
[362] H. Li, J. Zhu, C. Wang, et al., Int. J. Pharm. 587 (2020) 119649.
[363] W. Strzempek, E. Menaszek, B. Gil, Microporous Mesoporous Mater. 280 (2019) 264–270.
[364] F. Figueira, J.S. Barbosa, R.F. Mendes, S.S. Braga, F.A.A. Paz, Mater. Today 43 (2021) 84–98.
[365] Y. Wang, Y. Hu, Q. He, et al., Biosens. Bioelectron. 169 (2020) 112604.
[366] G.H. Qiu, Z.H. Weng, P.P. Hu, et al., Talanta 180 (2018) 396–402.
[367] L. Qin, L.X. Lin, Z.P. Fang, et al., Chem. Commun. 52 (2016) 132–135.
[368] Y.W. Zhang, W.S. Liu, J.S. Chen, et al., Sens. Actuator. B: Chem. 321 (2020) 128456.
[369] B.P. Xie, G.H. Qiu, P.P. Hu, et al., Sens. Actuator. B: Chem. 254 (2018) 1133–1140.
[370] L. Wang, K. Liang, W. Feng, et al., Microchem. J. 164 (2021) 106047.
[371] J. Yang, W. Feng, K. Liang, et al., Talanta 212 (2020) 120744.
[372] M.T. Marcos-Almaraz, R. Gref, V. Agostoni, et al., J. Mater. Chem B 5 (2017) 8563–8569.
[373] W. Hu, M.R. Younis, Y. Zhou, C. Wang, X. Xia, Small 16 (2020) 2000553.
[374] D. Mao, F. Hu, S. Kenry, et al., Adv. Mater. 30 (2018) 1706831.
[375] J.H. Jo, H.C. Kim, S. Huh, et al., Dalton. Trans. 48 (2019) 8084–8093.
[376] G. Wang, W. Jin, A.M. Qasim, Biomaterials 124 (2017) 25–34.
[377] Y. Zhang, P. Sun, L. Zhang, et al., Adv. Funct. Mater. 29 (2019) 1808594.
[378] W. Zhang, X. Ren, S. Shi, et al., Nanoscale 12 (2020) 16330–16338.
[379] W. Zhuang, D. Yuan, J.R. Li, et al., Adv. Healthc. Mater. 1 (2012) 225–238.
[380] X. Liu, Z. Yan, Y. Zhang, ACS Nano 13 (2019) 5222–5230.
[381] A.L. Sharabati, M. Sabouni, R. Husseini, Nanomaterials 12 (2022) 277.

[382] H. Xia, N. Li, X. Zhong, Y. Jiang, Front. Bioeng. Biotechnol. 8 (2020) 695.
[383] J. Yao, Y. Cheng, M. Zhou, et al., Chem. Sci. 9 (2018) 2927–2933.
[384] C. Hao, A. Qu, L. Xu, et al., J. Am. Chem. Soc. 141 (2019) 1091–1099.
[385] M. Lu, C. Wang, Y. Ding, et al., Chem. Commun. 55 (2019) 14534–14537.
[386] K.M. Holmstrom, T. Finkel, Nat. Rev. Mol. Cell Biol. 15 (2014) 411–421.
[387] R. Yan, S. Sun, J. Yang, et al., ACS Nano 13 (2019) 11552–11560.
[388] H. Liu, Y. Li, S. Sun, et al., Nat. Commun. 12 (2021) 114.
[389] D.D. Wang, Y. Zhao, Chemistry 7 (2021) 2635–2671.
[390] X. Wang, Y. Hu, H. Wei, Inorg. Chem. Front. 3 (2016) 41–60.
[391] J. Zhao, X. Cai, W. Gao, ACS Appl. Mater. Interfaces 10 (2018) 26108–26117.
[392] Y. Liu, Y. Cheng, H. Zhang, et al., Sci. Adv. 6 (2020) 1–10.
[393] H. Li, X. Cao, X. Fei, S. Zhang, Y. Xian, J. Mater. Chem. B 7 (2019) 3027–3033.
[394] J. Zhuang, H. Gong, J. Zhou, Sci. Adv. 6 (2020) 1–10.
[395] Q. Chen, M. Xu, W. Zheng, ACS Appl. Mater. Inter. 9 (2017) 6712–6724.
[396] X. Yang, Q. Tang, Y. Jiang, et al., J. Am. Chem. Soc. 141 (2019) 3782–3786.
[397] M.Z. Alyami, S.K. Alsaiari, Y. Li, et al., J. Am. Chem. Soc. 142 (2020) 1715–1720.
[398] K.X. Li, G.W. Guan, L.M. Pei, Q.Y. Yang, Mater. Chem. Front. 7 (2023) 2896–2905.
[399] W. Li, R. Wang, Z. Chen, J. Chromatogr. A 1607 (2019) 460403.
[400] H. Zhang, Z. Li, W. Shi, Prog. Chem. 35 (2023) 475.
[401] X. Liu, Y. Xie, M. Hao, Adv. Sci. 9 (2022) 2201735.
[402] S. Wang, Y. Li, Q. Liu, et al., J Photochem. Photobiol. A: Chem. 437 (2023) 114435.
[403] F. Xing, H. Ma, P. Yu, et al., Mater. Design. (2023) 112252.
[404] D. Wang, Y. Zhao, Chem. 7 (2021) 2635–2671.
[405] C. Keum, C.M. Hirschbiegel, S. Chakraborty, et al., Nano Convergen. 10 (2023) 1–41.
[406] J. Sun, X. Zhang, D. Zhang, et al., CCS Chem. 4 (2022) 996–1006.
[407] B.T. Liu, X.H. Pan, D.Y. Nie, et al., Adv. Mat. 32 (2020) 2005912.
[408] B.T. Liu, X.H. Pan, D.Y. Zhang, et al., Angew. Chem. Int. Ed. 60 (2021) 25701–25707.